REPORT DOCUMENTATION PAGE

AD-A256 015

1. AGENCY USE ONLY (Leave blank)	2. REPORT DATE	3. REPORT TYPE AND DATES COVERED
	92/6/11	Final Technical Report - 3/1/89 to 2/28/92

4. TITLE AND SUBTITLE
(U) Chemical Kinetic and Aerodynamic Structures of Flames

5. FUNDING NUMBERS
PE - 61102F
PR - 2308
SA - BS
G - 89-0293

6. AUTHOR(S)
C.K. Law

7. PERFORMING ORGANIZATION NAME(S) AND ADDRESS(ES)
Princeton University
Department of Mechanical and Aerospace Engineering
Princeton, NJ 08544

8. PERFORMING ORGANIZATION REPORT NUMBER
AFOSR-TR- 92 0[illegible]4

9. SPONSORING/MONITORING AGENCY NAME(S) AND ADDRESS(ES)
AFOSR/NA
Building 410
Bolling AFB DC 20332-6448

10. SPONSORING/MONITORING AGENCY REPORT NUMBER

11. SUPPLEMENTARY NOTES

12a. DISTRIBUTION/AVAILABILITY STATEMENT
Approved for public release; distribution is unlimited

12b. DISTRIBUTION CODE

13. ABSTRACT (Maximum 200 words)

The objective of the present program was to study the aerothermochemical structure of laminar premixed and nonpremixed flames through (a) non-intrusive experimental determination in reduced and elevated pressure environments, (b) computational simulation using detailed flame and kinetic codes, and (c) asymptotic analysis with simplified and reduced mechanisms. Useful theoretical and experimental contributions were made on the determination of the burning rates and flame kinetics of the lower hydrocarbons, on the understanding of the physical and chemical parameters influencing soot formation in diffusion flames, on the identification of the role of kinetics and system non-adiabaticity in flammability limits, and on adiabatic flame stabilization. These results are relevant to the fundamental and practical issues of flame kinetics, turbulent combustion, soot formation, radiative heat transfer, flame extinction, stabilization and flammability, and supersonic combustion.

92 10 [illegible]

14. SUBJECT TERMS
Flammability limit, flame extinction, hydrocarbon combustion, chemical kinetics, flame stabilization, soot formation, turbulent combustion.

15. NUMBER OF PAGES
55

16. PRICE CODE

17. SECURITY CLASSIFICATION OF REPORT	18. SECURITY CLASSIFICATION OF THIS PAGE	19. SECURITY CLASSIFICATION OF ABSTRACT	20. LIMITATION OF ABSTRACT
Unclassified	Unclassified	Unclassified	UL

SUMMARY/OVERVIEW

The objective of the present program is to study the aerothermochemical structure of laminar premixed and nonpremixed flames through (a) non-intrusive experimental determination in reduced and elevated pressure environments, (b) computational simulation using detailed flame and kinetic codes, and (c) asymptotic analysis with simplified and reduced mechanisms. Useful theoretical and experimental contributions have been made on the determination of the flame burning rates and flame kinetics of the lower hydrocarbons, on the understanding of the physical and chemical parameters influencing soot formation in diffusion flames, on the identification of the role of kinetics and system nonadiabaticity in flammability limits, and on adiabatic flame stabilization. These results are expected to be useful in the general interest of AFOSR in the fundamental and practical issues of flame kinetics, turbulent combustion, soot formation, radiative heat transfer, flame extinction, stabilization and flammability, and supersonic combustion.

ACCMPLISHMENTS

The highlights of our accomplishments can be found in the annual reports submitted to the program director, as well as the journal papers which have either appeared or have been accepted for publication. Thus only a very brief summary of those completed works of archival value are discussed in the following.

1. Determination of Burning Velocities and Chemical Kinetics of Hydrocarbon/Air Mixtures

A major accomplishment of our AFOSR program has been the development of the counterflow twin flame technique which allows the accurate determination of the laminar flame speeds of combustible mixtures. Basically, practically all existing techniques for the determination of laminar flame speeds impart stretch and/or heat loss effects on the data obtained, causing significant and systematic spreads in their values. Thus when such flame speed data are used to calibrate or validate chemical kinetic

mechanisms and rate constants, the fundamental chemical information so determined can be significantly "contaminated" or even falsified. In the technique we proposed, such effects can be systematically subtracted out, yielding flame speed data of unusual fidelity.

For the present grant period, we have capitalized on our expertise in this area in the study of a variety of fuel/oxidizer systems. First, we have extended our previous study of methane/air flames to cover all the C_2 hydrocarbon fuels of ethane, ethylene, and acetylene, as well as propane. Such an extension is crucial because methane only has the C-H bonds although the breaking of the C_2 bonds is important in the kinetics of all of the higher hydrocarbons. Through this study we have found that all existing C_2 kinetic schemes are inadequate to describe our experimental results. Consequently a new kinetic scheme which was able to correlate practically all of our experimental results was proposed. It is also important to mention that, through our effort over the years, there now exist reliable experimental flame speed data for methane, ethane, ethylene, acetylene, and propane, determined over extensive ranges of stoichiometry and up to pressures of about 3 atmospheres. These data are essential for both fundamental and practical studies. This work is reported in Publication No.1.

We have also studied the oxidation kinetics of hydrogen. The practical interest to AFOSR is on supersonic combustion, while the fundamental interest is that hydrogen oxidation forms a fundamental building block for the oxidation of carbon dioxide as well as the hydrocarbons. In this study we have focused on very lean mixtures because flame speed data for these situations do not exist, and because of the interest in low- and intermediate-temperature kinetics which control these weakly-burning flames. In may be noted that previous studies on very lean hydrogen/air flames have all been complicated by the presence of flamefront instabilities which are favored to occur for these high Lewis number flames. However, since such instabilities are suppressed by the positively strained flow field of the counterflow flame, we have succeeded in obtaining data for smooth hydrogen/air flames. Our experimental results show that there is something seriously wrong with the existing hydrogen/oxygen kinetics, in these low flame temperature regimes, in that the predicted flame response obtained by using existing mechanisms completely fails to predict the observed behavior even qualitatively. It seems that the actual kinetics is more robust than indicated. This could be caused

by the great uncertainty associated with the kinetics involving the HO_2 and H_2O_2 radicals, as generally acknowledged by the chemical kinetics community. This work is reported in Publication No.2.

In an effort to further scrutinized the kinetics of HO_2 and H_2O_2, we have performed additional experiments on methanol oxidation, for which these radicals are expected to exert different influences. Some useful insights have been gained, although the issue of hydrogen oxidation remains. The work on methanol oxidation is reported in Publication No.3.

The laminar flame speed data we have been reporting over the past few years have now enjoyed wide popularity among combustion kineticists and flame modellers. Since these data are scattered in various journal papers and also reported in different formats, upon request from many of our colleagues we have consolidated and re-plotted all our data in a uniform format. The compilation is reported in Publication No. 4, which will appear in a monograph on reduced mechanisms. All contributors to this monograph are asked to compare their calculated results against our reported flame speeds.

We next note that in efforts to describe the effects of chemical reaction on combustion phenomena with greater realism than the one-step reaction frequently used in theoretical analysis, various reduced mechanisms based on steady-state and partial equilibrium concepts have been developed. Most of these mechanisms consist of four steps. We have, however, found that these four-step mechanisms are not adequate to describe the computed flame responses using detailed chemical mechanisms. The deficiency was identified to be the steady-state assumption for the CH_3 radical. A five-step mechanism was subsequently proposed, and the agreement was significantly improved. This result is expected to be of particular relevance to phenomena that are strongly dependent on accurate descriptions of the CH_3 such as the formation of prompt NO_x and fuel rich combustion. This work is reported in Publication No. 5.

In another work of great interest, by using the laminar flame speed data for methane/air mixtures we have extracted the kinetic parameters of the reaction order (n) and activation energy (E) for the equivalent one-step overall reaction. The results show that these values are far from being constants. Instead they vary significantly not only with the equivalence ratio, but also with the system pressure. For example, the activation energy is

found to continuously increase with pressure. The reaction order is found to be just about one at atmospheric pressure and decreases with increasing pressures. For highly-diluted environments n can even assume negative values. Such behavior can be explained on the basis of the competition between termination and branching reactions. This work is reported in Publication No. 6.

The above work are all concerned with premixed flames. We have in addition also performed extinction experiments on methane/air diffusion flames. The extinction stretch rates were consequently determined as a function of local stretch measured by LDV. The data were then compared with numerical simulations and useful insight into the extinction mechanism were gained. This work is reported in Publication No. 5.

We close this section by emphasizing the significance of our contributions in the area of fundamental flame and kinetics research. At the 23rd International Combustion Symposium, the principal investigator was awarded the Combustion Institute Silver Medal for the development of the counterflow twin-flame technique for the determination of the laminar flame speed.

2. Theory of Flammability Limits

Although the term "flammability limit" has been extensively used in the combustion literature, its real meaning has remained unclear and undefined. Thus a *major* and *sustained* undertaking of the present program is to understand the phenomenon of flammability limits and to be able to predict their values from first principles. Through various considerations, we have argued that a truly fundamental definition of flammability limits should be related to the state at which the classical one-dimensional planar flame fails to propagate, as originally adopted by Spalding in his attempt to define such a limit. By introducing a volumetric heat loss rate into the energy equation, and by assuming a one-step overall reaction as well as conventional transport properties, subsequent analytic solutions yield an extinction state in terms of a turning point response of the mass burning rate to increasing heat loss, indicating the incipient loss of balance between heat loss and chemical heat generation. It is further shown that the ratio of the limit flame speed to the adiabatic flame speed is $e^{-1/2}=0.61$.

The loss theory is inherently incapable of explaining the chemical kinetic dependence of the flammability limits, in terms of the frequently-present chain branching and termination mechanisms, on such system parameters as pressure, stoichiometry, and fuel type. In Publication No. 8 we first proposed a chain-based approach, in which it was argued that competition between chain branching and termination reactions must be important to the weakly-reactive flames close to the flammability limits. Thus by numerically simulating the one-dimensional flame propagation with detailed chemistry and transport properties, but without radiative heat loss, a normalized sensitivity coefficient of the termination reaction to variations in the branching reaction can be calculated. This coefficient, termed the flammability exponent, was found to assume a value close to unity in the vicinity of the experimentally-observed flammability limits of a great variety of mixtures.

It is clear that the heat loss theory of Spalding and our chain branching-termination criterion are based on completely different concepts and approaches, and that neither one is complete. These two concepts have since been unified in Publication No. 9. The approach towards such a unified treatment, with quantitative accuracy, is to numerically simulate the freely-propagating, one-dimensional flame with detailed chemistry and diffusive properties, allowing for radiative heat loss from the major species, and to generate the characteristic turning point. At the same time, the relative efficiencies of the key termination versus branching reactions will be assessed through the concept of the flammability exponent, especially near and at the state of the turning point.

Calculations have been conducted for lean methane/air and rich hydrogen/air flames with and without radiative heat loss. The results show that the nonadiabatic flame indeed exhibits a turning point. At the turning point, the flame speed and temperature are very close to those predicted from asymptotic theories when referenced to the adiabatic values, which are well established. It is further shown that the flammability exponent assumes a value close to unity at the turning point.

The above results provide a unified interpretation of flammability limits by recognizing that the influence of heat loss and chain termination on flame propagation become critical almost simultaneously. As such, flammability limits determined through the turning point behavior are

almost identical to those determined through the unity flammability exponent criterion. The result is entirely physically reasonable by considering the following. As the flammability limit is approached, the adiabatic flame temperature is reduced due to the change in stoichiometry. This weakens the temperature sensitive two-body branching reaction but usually has a much weaker influence on the termination reactions, especially when it involves three bodies. Therefore, a state will be reached at which the termination reaction becomes overwhelmingly strong, as indicated by the unity flammability exponent, and consequently causes a rapid slow down of the overall reaction rate and thereby the overall heat release rate. This, in turn, makes the influence of heat loss relatively severe, and therefore simultaneously results in the extinction turning point.

3. Soot Formation in Diffusion Flames

We have completed two projects related to soot formation in diffusion flames. In the first project, we have continued our study of the influence of dilution on soot formation. As background, we note that a major concept developed in recent studies on soot formation in diffusion flames is that the flame temperature exerts a dominant influence on soot formation. This concept has been experimentally investigated by lowering the flame temperature by diluting the fuel stream with an inert. We have, however, argued that since the act of dilution not only lowers the flame temperature but also its concentration, this concentration modification should also have an effect on soot formation. By subsequently conducting the experiment by holding either the flame temperature or the fuel concentration fixed, we have shown that not only temperature and concentration are equally important in soot formation, in many instances dilution can be even more important.

Our previous experiments were conducted by using the counterflow flame, although most of the literature experiments were performed with the co-flow flame. We have therefore repeated our experimental investigation for the co-flow flame, using the same isolation technique as developed previously. The results confirm our previous finding of the simultaneous importance of temperature and concentration in soot formation. This work is reported in Publication No.10.

Our second project on soot formation involves the influence of additives. Carbon monoxide and oxygen were added to either the fuel or the oxidizer side of a diffusion flame, and the chemical, dilution, and temperature effects were isolated and studied. Results show that the addition of carbon dioxide is usually suppressive, while the addition of oxygen can be either promoting or suppressive. This work is reported in Publication No.11.

4. Adiabatic Flame Stabilization

The mechanism with which a Bunsen flame is stabilized at the burner rim is considered to be well established. The concept of stabilization is based on the existence of a dynamic balance between the local flow velocity and flame velocity at a certain point on the flame surface, and the ability of the flame to adjust its flame velocity, and thereby the location of stabilization, through heat loss to the rim. Blowoff occurs when such a balance can not be achieved everywhere on the flame surface. This mechanism has also served as the fundamental concept in flame stabilization through heat loss to the stabilization body in other practical situations.

However, recent studies on the dynamics of stretched flames have shown that, in addition to heat loss, the flame speed can also be modified by flow nonuniformity, flame curvature, and mixture preferential diffusion. It is, therefore, of interest to explore the possibility that flame stabilization can be achieved in the absence of heat loss due to these additional mechanisms. The configuration adopted for study is the inverted flame because of its symmetry. By measuring the temperature distribution in the stabilization region, we conclusively demonstrated that the flame can indeed be stabilized in the absence of heat loss. We subsequently formulated a theory that satisfactorily describes the stabilization of this adiabatic flame through the combined influence of flow nonuniformity and flame curvature.

It may be emphasized that the concept and methodology developed in this study will be useful in future studies of flame stabilization in combustors, as well as the quenching of laminar flamelets constituting turbulent flames.

This work is reported in Publication No. 12.

5. Review Activities

A review article on subsonic and supersonic flame stabilization, listed as Publication No.13, was prepared and presented at a workshop on supersonic combustion at NASA Langley Research Center.

JOURNAL PUBLICATIONS

1. "Experimental and Numerical Determination of Laminar Flame Speeds: Mixtures of C_2-Hydrocarbons with Oxygen and Nitrogen," by F.N. Egolfopoulos, D.L. Zhu and C.K. Law, *Twenty-Third Symposium (International) on Combustion*, The Combustion Institute, Pittsburgh, PA, pp.471-478 (1991).

2. "An Experimental and Computational Study of the Burning Rates of Ultra-Lean to Moderately-Rich $H_2/O_2/N_2$ Laminar Flames with Pressure Variations," by F.N. Egolfopoulos and C.K. Law, *Twenty-Third Symposium (International) on Combustion*, The Combustion Institute, Pittsburgh, PA, pp.333-340 (1991).

3. "A Comprehensive Study of Methanol Kinetics in Freely-Propagating and Burner-Stabilized Flames, Flow and Static Reactors, and Shock Tubes," by F.N. Egolfopoulos and C.K. Law, *Combustion Science and Technology* **83**, pp. 33-75 (1992).

4. "A Compilation of Experimental Data on Laminar Burning Velocities," by C.K. Law, to appear in *Reduced Kinetic Mechanisms for Application in Combustion*, (Ed.: B.Rogg and N. Peters), Springer-Verlag.

5. "Reduced Kinetic Mechanisms for Counterflow Methane-Air Diffusion Flames," H. Chelliah, K, Seshadri and C.K. Law, to appear in *Reduced Kinetic Mechanisms for Application in Combustion*, (Ed.: B.Rogg and N. Peters), Springer-Verlag.

6. "Chain Mechanisms in the Overall Reaction Order in Laminar Flame Propagation," by F.N. Egolfopoulos and C.K. Law, *Combustion and Flame* **80**, pp.7-16, (1990).

7. "An Experimental and Theoretical Investigation of the Dilution, Pressure and Flow-Field Effects on the Extinction Condition of Methane-Air-Nitrogen Diffusion Flames," by H.K. Chelliah, C.K. Law, T. Ueda, M.Smooke and F.A. Williams, *Twenty-Third Symposium (International) on Combustion*, The Combustion Institute, Pittsburgh, PA, pp.503-511 (1991).

8. "A Kinetic Criterion of Flammability Limits: The C-H-O-Inert System," by C.K. Law and F.N. Egolfopoulos,*Twenty-Third Symposium (International) on Combustion*, The Combustion Institute, Pittsburgh, PA, pp.413-421 (1991).

9. "A Unified Chain-Thermal Theory of Fundamental Flammability Limits," by C.K. Law and F.N. Egolfopoulos, to appear in *Proc. of Twenty-Fourth Symposium (International) on Combustion*, The Combustion Institute.

10. "Soot Formation and Inert Addition in Diffusion Flames," by R.L. Axelbaum and C.K. Law, *Twenty-Third Symposium (International) on Combustion*, The Combustion Institute, Pittsburgh, PA, pp.1517-1523 (1991).

11. "The Influence of Carbon Dioxide and Oxygen as Additives on Soot Formation in Diffusion Flames," by D.X. Du, R.L. Axelbaum and C.K. Law, *Twenty-Third Symposium (International) on Combustion*, The Combustion Institute, Pittsburgh, PA, pp.1501-1507 (1991).

12. "On Adiabatic Stabilization of Inverted Flames," by C.J. Sung, C.K. Law and A. Umemura, to appear in *Proc. of Twenty-Fourth Symposium (International) on Combustion*, The Combustion Institute.

13. "Mechanisms of Flame Stabilization in Subsonic and Supersonic Flows," by C.K. Law, *Major Research Topics in Combustion* (Eds.: M.Y. Hussaini, A. Kumar and R.G. Voigt), Springer-Verlag, pp. 201-236 (1992).

PRESENTATIONS

1. "Extinction and Flammability of Gaseous Combustibles," Department of Mechanical Engineering, Yale University, New Haven, CT, Feb. 22, 1989.

2. "Extinction and Flammability of Gaseous Combustibles," Department of Mechanical Engineering, Pennsylvania State University, University Park, PA, March 16, 1989.

3. "Extinction Mechanisms in Premixed Flames," Department of Mechanical Engineering and Mechanics, Drexel University, Philadelphia, PA, April 6, 1989.

4. "Structure, Stabilization and Propagation of Laminar Premixed Flames," Department of Chemical Engineering, Illinois Institute of Technology, Chicago, IL, Sept. 9, 1989.

5. "Mechanisms of Ignition, Extinction and Flame Stabilization in Subsonic and Supersonic Flows," Workshop on Supersonic Combustion, NASA Langley Research Center, Hampton, VA, Oct. 2-4, 1989. **Invited Position Paper**

6. "Combustion in Microgravity: Opportunities, Challenges, and Progress," AIAA Aerospace Science Meeting, Reno, Nevada, Jan. 8-12, 1990. **Keynote Paper**

7. "Mechanisms of Extinction, Stabilization, and Flammability of Premixtures," Hotel Lecture, Massachusetts Institute of Technology, Cambridge, MA, Oct. 25, 1990.

8. "Extinction, Stabilization, and Flammability in Premixed Systems," Department of Applied Mechanics and Engineering Sciences, University of California at San Diego, CA, Feb. 7, 1991.

9. "Extinction, Stabilization, and Flammability in Premixed Systems," Department of Mechanical Engineering, University of California at Irvine, CA, Feb. 7, 1991.

10. "Combustion in Microgravity," U.S.-Taiwan Workshop on Space Processing, Taipei, Taiwan, April 16, 1991. **Invited Talk**

11. "Extinction, Stabilization and Flammability in Combustion Systems," Department of Power Mechanical Engineering, National Tsing Hua University, Hsinchu, Taiwan, April 22, 1991.

12. "Extinction, Stabilization and Flamability in Combustion Systems," Department of Mechanical Engineering, National Taiwan University, Taipei, Taiwan, April 23, 1991.

13. "Extinction, Stabilization and Flamability in Combustion Systems," Department of Mechanical Engineering, University of Sydney, Sydney, Australia, June 18, 1991.

14. "A Kinetic Criterion of Flammability Limits: The C-H-O-Inert System," Twenty-Third Symposium (International) on Combustion, Orlean, France, July 22-27, 1990.

PROFESSIONAL PERSONNEL

1. C. K. Law: Principal Investigator
2. H. K. Chelliah: Research Staff
3. R. L. Axelbaum: Post-Doctoral Fellow
4. F. N. Egolfopoulos: Graduate Student and then Post-Doctoral Fellow
5.. C. J. Sung: Graduate Student
6. D. L. Zhu: Technical Staff
7. D. X. Du: Visiting Scholar
8. T. Ueda: Visiting Scholar
9. A. Umemura: Visiting Scholar

SIGNIFICANT INTERACTION

The laminar flame speed data that have been experimentally determined in the P.I.'s laboratory have now been extensively adopted by chemical kineticists in their modeling efforts.

INVENTIONS

None.

Combust. Sci. and Tech., 1992, Vol. 83, pp. 33-75
Photocopying permitted by license only

A Comprehensive Study of Methanol Kinetics in Freely-Propagating and Burner-Stabilized Flames, Flow and Static Reactors, and Shock Tubes

F. N. EGOLFOPOULOS, D. X. DU and C. K. LAW *Department of Mechanical and Aerospace Engineering, Princeton University, Princeton, NJ 08544*

(*Received April 9, 1991; in final form August 5, 1991*)

Abstract—An experimental and numerical study of methanol kinetics has been conducted. A detailed kinetic scheme was compiled which closely predicts properties of mixtures of methanol, oxygen, and inert for a variety of experimental configurations and conditions. The scheme incorporates the most recent kinetic information and was tested against experimental data for the propagation speeds and structure of laminar flames as well as the species concentration evolutions in flow reactors, static reactors, and shock tubes. The laminar flame speeds of atmospheric methanol/air mixtures were determined using the counterflow flame technique over extensive lean-to-rich fuel concentration ranges and for initial mixture temperatures ranging from 318 to 368 K, while the experimental data on the laminar flame structure and from reactors and shock tubes were obtained from the literature. The scheme compiled herein includes the detailed C_1, C_2, and methanol submechanisms and yields close agreement with all of the experimental methanol/air laminar flame speeds as well as previously determined laminar flame speeds of mixtures of CH_4 and the C_2-hydrocarbons with air. The relative importance and influence of the individual reactions on the flame speed and reaction mechanism were assessed with the aid of sensitivity and species consumption path analyses. The study also demonstrates that accurate prediction of laminar flame speeds is only a necessary but not sufficient condition for the validation of the mechanism, and that results from the flame structure as well as reactors and shock tubes are also needed for further validation. Both flow and static reactor oxidation studies indicate that the reaction $CH_3OH + OH \rightarrow$ Products may have a slower rate than that reported in recent literature.

1 INTRODUCTION

In the search of viable alternate fuels for reduced pollutant emissions and lessened dependence on available petroleum supplies, alcohols and their blends with conventional petroleum stocks are among the strongest candidates. In particular, methanol, the simplest of the alcohols, has been the subject of extensive laboratory and road testing studies as well as legislative directives encouraging its use.

There are various advantages and disadvantages in the use of methanol as a practical fuel (Bowman, 1975; Aronowitz *et al.*, 1979; Westbrook and Dryer, 1979; Gülder, 1982; Dove and Warnatz, 1983; Cribb *et al.*, 1984; Grotheer and Kelm, 1989; Norton and Dryer, 1989, 1990; Norton, 1990). Specifically, the major advantages are: (a) convenient storage in vehicles as a liquid fuel under normal temperature and pressure, (b) diversified, petroleum-independent sources of production, such as natural gas, wood, coal, and renewable biomass feedstock, (c) reduced propensity for the formation of pollutants such as soot, CO, NO_x, and unburned hydrocarbons, and (d) high octane number rating. Among the various disadvantages (Norton, 1990) are: (a) lower energy density, (b) propensity to form formaldehyde, (c) infinite miscibility with water and thereby tendency to dissolve atmospheric moisture, and (d) low vapor pressure leading to cold start problems typically below 15°C.

Satisfactory studies of methanol combustion, at both the fundamental and practical levels, require a good understanding of the chemical kinetics of its oxidation and the associated pyrolysis steps. Early attempts to model methanol oxidation were fraught with significant uncertainty until Tsang (1987) compiled an extensive chemical

data base for methanol-related reactions, with a rigorous evaluation of all available data. Based on this data base, Norton and Dryer (1989, 1990) revised the previous scheme of Westbrook and Dryer (1979) to analyze their recent flow reactor data as well as published data obtained from static reactors and shock tubes. The fundamental understanding gained from these studies is that, compared to the oxidation of methane, the presence of the C–O bond in the methanol molecule significantly alters its kinetic behavior in that completely different kinetic paths are being followed after the initial fuel reactions. As such, the current extensive knowledge of the C_1 and C_2 chemistry developed for methane oxidation is intrinsically inadequate to describe methanol oxidation. It is, however, also recognized that although significant advances in the understanding of methanol kinetics have been achieved from these worthwhile studies, more validation studies over wider temperature, concentration, and pressure ranges are needed, especially for some of the crucial kinetic steps involving intermediates such as CH_2OH, CH_3O, CH_2O, and HCO.

Such additional validations can be achieved through simulation of flame propagation and structure because of the extensive variations in the temperature and species concentrations across the flame. Methanol flames have been the subject of a number of experimental and numerical investigations (Wiser and Hill, 1955; Henderson and Hill, 1956; Gibbs and Calcote, 1959; De Wilde and Van Tiggelen, 1968; Akrick *et al.*, 1978; Westbrook and Dryer, 1979, 1980; Westbrook, 1980; Hirano *et al.*, 1981; Vandooren and Van Tiggelen, 1981; Gülder, 1982; Metghalchi and Keck, 1982; Dove and Warnatz, 1983; Anderson *et al.*, 1984; Olsson *et al.*, 1986, 1987; Grotheer and Kelm, 1989; Pauwels *et al.*, 1989, 1990; Bradley *et al.*, 1991) and certain rates have been determined and/or adjusted based on comparisons between experiments and calculations. The fidelity of such simulations, however, depends on the accuracy of the experimental data. Specifically, it is generally recognized (Law, 1989) that while the numerical simulation employs the one-dimensional planar configuration, the experimental flame/flow configurations can deviate significantly from such an idealized prescription and consequently suffer substantial, and frequently unquantified, flame stretch effects. To demonstrate this point, the limited experimental data on the laminar flame speeds, S_u^0, of methanol/air flames under 1 atmosphere pressure and initial mixture temperature, T_u, of 298 K (Wiser and Hill, 1955; Gibbs and Calcote, 1959; Gülder, 1982; Metghalchi and Keck, 1982) are compiled in Figure 1 together with the present experimental results; note that S_u^0 has been conventionally termed the burning rate of the mixture. It is seen that these data not only depend on the specific technique used, whether flame tube (Wiser and Hill, 1955), Bunsen flame (Gibbs and Calcote, 1959), and constant volume bomb (Gülder, 1982; Metghalchi and Keck, 1982), but there is also systematic difference between data determined by the same technique (Gülder, 1982; Metghalchi and Keck, 1982). The spread of these data is sufficiently wide as to cause concern in the assessment of the rate constants of various crucial reactions.

In view of the above considerations, the first objective of the present investigation is to provide experimental data of improved accuracy on S_u^0 for atmospheric methanol/air flames over extensive ranges of stoichiometry and for several initial mixture temperatures. The technique used is that of the counterflow twin flame, with systematic elimination or minimization of stretch effects (Wu and Law, 1985; Yu *et al.*, 1986; Egolfopoulos *et al.*, 1989; Law, 1989; Zhu *et al.*, 1989; Egolfopoulos *et al.*, 1990, 1991). The availability of these data is essential not only for the present kinetic studies but also for simulation studies of more complex fundamental and practical systems.

The second objective is to compare our experimental S_u^0 data with the numerically-

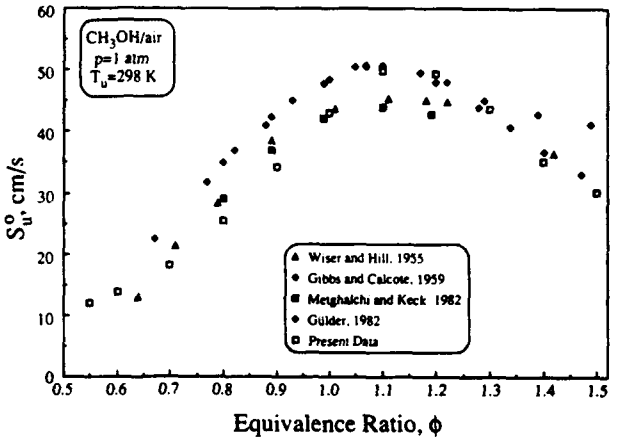

FIGURE 1 Experimental laminar flame speeds, $S_u^0(\phi)$, for methanol/air mixtures at $T_u = 298$ K and $p = 1$ atm, from various sources.

calculated values by grafting the mechanol submechanism of Norton and Dryer (1989, 1990) onto a previously developed C_2 kinetic scheme (Egolfopoulos *et al.*, 1990, 1991) which closely predicts the laminar flame speeds of mixtures of CH_4 and the C_2-hydrocarbons with O_2 and N_2. These comparisons will be used to assess the validity of existing rate coefficients through sensitivity and species consumption path analyses. Such a comparison will also demonstrate that agreement in the laminar flame speed is a necessary but not sufficient condition for the validation of a kinetic scheme, and that additional comparisons are needed.

This then leads to the third objective, which is to further test the proposed mechanism against a wide variety of experimental data found in the literature on the laminar flame structure obtained from flat-flame burners, and on the homogeneous reaction processes obtained from flow reactors, static reactors, and shock tubes. These additional comparisons cover temperatures from 820 to 2180 K, pressures from 0.05 to 4.7 atmospheres, and stoichiometries from very fuel lean ($\phi = 0.05$) to fuel pyrolysis conditions. It will be shown that the important reactions can differ for the different experimental techniques, thereby demonstrating the importance of utilizing all available information for the comprehensive validation of a proposed kinetic mechanism, as originally emphasized by Westbrook and Dryer (1979).

In the following we shall first define the experimental and numerical aspects of the present investigation. This will be followed by comparison and discussion of the results from the various studies involving the laminar flame speeds, the structure of burner-stabilized flames, the flow reactor, the static reactor, and the shock tube.

2 EXPERIMENTAL METHODOLOGY

The counterflow twin flame technique for the determination of laminar flame speeds is well documented (see *e.g.*, Egolfopoulos *et al.*, 1989; Zhu *et al.*, 1989). It involves the establishment of two symmetrical, planar, nearly-adiabatic flames in a nozzle-generated counterflow configuration, and the subsequent determination of the axial velocity profile along the centerline of the flow by laser Doppler velocimetry. The minimum point of the velocity profile is identified as a reference upstream flame speed, S_u, while the velocity gradient ahead of this point characterizes the imposed stretch

rate, K. Thus by plotting S_u *vs* K, the stretch-free flame speed S_u^0 is obtained through linear extrapolation to zero stretch.

The main difference between the present and the previous investigation is that a liquid rather than a gaseous fuel was used, hence necessitating the inclusion of a continuous-flow evaporator which vaporizes and mixes the methanol with preheated air. The air was filtered and preheated by passing through an electrically-heated copper tube, while methanol vaporization was achieved by injecting and impinging a liquid jet on a hot plate. All flow lines were electrically-heated in order to avoid subsequent condensation. In addition, the inner surface of a burner was heated with a continuous flow of hot water through a surrounding jacket. The unburned mixture temperature, T_u, was measured with a thermocouple at the exit of the nozzle. This temperature was controlled by the heating rates of the air and the internal surfaces of the burners, and was sufficiently high to ensure that methanol remains in the gaseous phase for all concentrations within the flammable range. The flow rates of methanol and air were respectively measured by using calibrated flowmeters and sonic orifices from which the mixture stoichiometry could be determined. The stoichiometry was further verified through independent gas chromatographic analyses of samples taken at the exit of the nozzle. Agreements were obtained for all cases. Further noting that steady state was maintained during the several hours of continuous experimentation, it was ensured that there was no liquid accumulation in the flow system.

3 NUMERICAL METHODOLOGY

Numerical simulation of all systems were conducted by using CHEMKIN-based programs (Kee *et al.*, 1983; Kee *et al.*, 1985; Lutz *et al.*, 1987; Kee *et al.*, 1989a) and the thermodynamic data base developed by Kee *et al.* (1987).

For the laminar flame speed determination, the freely-propagating flame version of the one-dimensional code (Kee *et al.*, 1985; Grcar *et al.*, 1986) was used, while for the laminar flame structure the burner-stabilized option of the code was used. Thermal diffusion was included in both cases. The code uses a hybrid time-integration/Newton-integration technique to solve the steady-state conservation equations of species and energy, and outputs the complete flame structure and the sensitivities of all reaction rates on the dependent parameters.

For the simulation of flow reactors, static reactors, and shock tubes, the SENKIN code (Lutz *et al.*, 1987) was used which predicts homogeneous gas phase chemical kinetics by integrating the time dependent conservation equations of species and energy. The code was also modified in order to include the option of constant volume and temperature reactions which is relevant to static reactor studies.

Detailed information on the use of the codes as well as comments on the validity of the comparisons for each case will be given in the following sections.

4 STUDIES BASED ON LAMINAR FLAME SPEEDS

The experimentally determined laminar flame speeds, S_u^0, of methanol/air mixtures at atmospheric pressure and for unburned mixture temperatures, T_u, of 318, 340, and 368 K are shown in Figure 2 for a wide range of stoichiometry. Figure 3 shows the anticipated result that S_u^0 basically increases linearly with T_u for all concentrations. Flame speeds at 298 K were not measured but were obtained by extrapolating the data at higher T_u to 298 K. As such they should be treated with some caution.

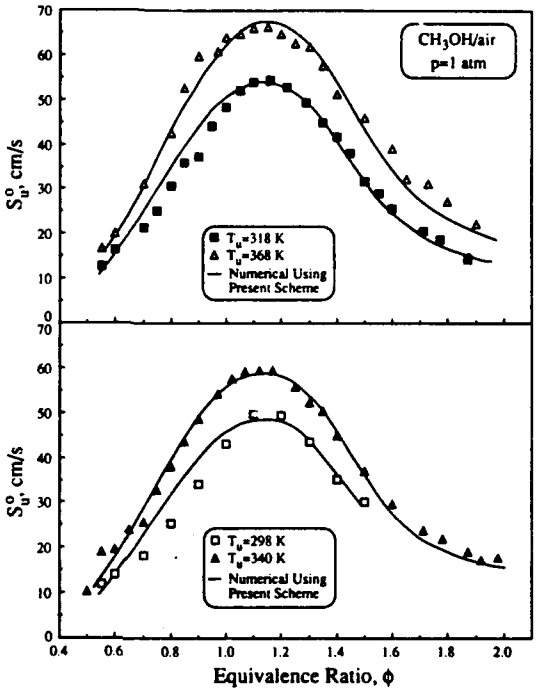

FIGURE 2 Experimentally and numerically determined laminar flame speeds, $S_u^0(\phi, T_u)$, at $p = 1$ atm, using the present kinetic scheme.

The maximum S_u^0 for methanol/air is found to occur around $\phi = 1.15$, which is higher than the corresponding value of $\phi = 1.05$ for methane/air. The reason for such a difference is the existence of the extra O atom in the methanol molecule which provides an additional amount of "oxidizer" as the fuel concentration becomes richer.

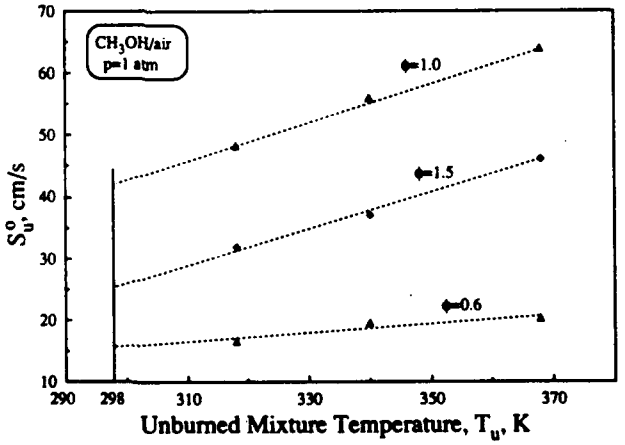

FIGURE 3 Experimentally determined laminar flame speeds, S_u^0, with T_u for lean, stoichiometric, and rich methanol/air flames at $p = 1$ atm, and the determination of S_u^0 at $T_u = 298$ K through linear extrapolation.

TABLE I

Present kinetic scheme describing the oxidation of CH_3OH and C_1- and C_2-hydrocarbons[a]

Reaction	Forward rate[b]			Backward rate			Reference
	A	β	E_a	A	β	E_a	
1. $H + O_2 = O + OH$	191E14	0.00	16440	3.72E11	0.44	−840	(Yetter *et al.*, 1990)
2. $O + H_2 = H + OH$	5.01E04	2.67	6290	3.57E04	2.61	4548	(Yetter *et al.*, 1990)
3. $OH + H_2 = H + H_2O$	6.38E06	2.00	2959	2.63E08	1.73	18750	(Yetter *et al.*, 1990)
4. $OH + OH = O + H_2O$	2.10E08	1.40	−397	1.22E10	1.19	17135	(Yetter *et al.*, 1990)
5. $H_2 + M = H + H + M$	4.57E19	−1.40	104380	4.79E19	−1.58	473	(Yetter *et al.*, 1990)
Enhanced third-body efficiencies[d]: H_2/2.5/ H_2O/16.0/ CO/1.9/ CH_4/16/ CH_3OH/5/							
6. $O + O + M = O_2 + M$	6.17E15	−0.50	0	2.15E18	−0.82	119388	(Yetter *et al.*, 1990)
Enhanced third-body efficiencies[d]: H_2/2.5/ H_2O/16.0/ CO/1.9 CO_2/3.8/ CH_4/16/ CH_3OH/5/							
7. $O + H + M = OH + M$	6.20E16	−0.60	0	4.22E16	−0.48	102115	(Glarborg *et al.*, 1986)
Enhanced third-body efficiencies[d]: H_2/5.0/							
8. $H + OH + M = H_2O + M$	2.19E22	−2.00	0	8.62E23	−2.09	119647	(Yetter *et al.*, 1990)
Enhanced third-body efficiencies[d]: H_2/2.5/ H_2O/16.0/ CO/1.9/ CO_2/3.8/ CH_4/16/ CH_3OH/5/							
9. $H + O_2 + M = HO_2 + M$	6.70E19	−1.42	0	8.75E20	−1.70	50018	(Slack, 1977)
Enhanced third-body efficiencies[d]: H_2/2.5/ H_2O/0.0/ CO/1.9/ CO_2/3.8/ CH_4/16/ CH_3OH/5/							
10. $H + O_2 + H_2O = HO_2 + H_2O$	6.89E15	0.00	−2085	9.00E16	−0.29	47934	(Hsu *et al.*, 1989)
11. $HO_2 + H = H_2 + O_2$	6.61E13	0.00	2130	4.83E12	0.46	55965	(Yetter *et al.*, 1990)
12. $HO_2 + H = OH + OH$	1.66E14	0.00	870	1.68E10	0.84	35695	(Yetter *et al.*, 1990)
13. $HO_2 + O = OH + O_2$	1.74E13	0.00	−400	9.06E11	0.40	51698	(Yetter *et al.*, 1990)
14. $HO_2 + OH = H_2O + O_2$	1.45E16	−1.00	0	4.37E16	−0.81	69629	(Yetter *et al.*, 1990)
15. $HO_2 + HO_2 = H_2O_2 + O_2$	3.02E12	0.00	1390	3.25E14	−0.35	39020	(Yetter *et al.*, 1990)
16. $H_2O_2 + M = OH + OH + M$	1.20E17	0.00	45500	8.67E09	1.48	−7346	(Yetter *et al.*, 1990)
Enhanced third-body efficiencies[d]: H_2/2.5/ H_2O/16.0/ CO/1.9/ CO_2/3.8/ CH_4/16/ CH_3OH/5/							
17. $H_2O_2 + H = H_2O + OH$	1.00E13	0.00	3590	2.84E07	1.39	70411	(Yetter *et al.*, 1990)
18. $H_2O_2 + H = H_2 + HO_2$	4.79E13	0.00	7950	3.26E10	0.81	24152	(Yetter *et al.*, 1990)
19. $H_2O_2 + O = OH + HO_2$	9.55E06	2.00	3970	4.62E03	2.75	18435	(Yetter *et al.*, 1990)

20. $H_2O_2 + OH = H_2O + HO_2$	7.08E12	0.00	1430	1.98E11	0.54	33427	(Yetter *et al.*, 1990)
21. $CH_4(+M) = CH_3 + H(+M)$	3.71E17	−0.558	104825	3.88E13	−0.03	−1727	(Stewart *et al.*, 1989)
Low pressure limit:	8.06E31	−3.732	106441	8.42E27	−3.20	−112	
SRI parameters: 0.34 797 979 1							
Enhanced third-body efficiencies[d]:							
H_2/2.5/ H_2O/16.0/ CO/1.9/ CO_2/3.8/ CH_4/16/ CH_3OH/5/							
22. $CH_4 + H = CH_3 + H_2$	2.25E04	3.00	8750	2.24E00	3.70	6101	(Tsang and Hampson, 1986)
23. $CH_4 + O = CH_3 + OH$	1.20E09	1.50	8599	8.53E04	2.15	4211	(Tsang and Hampson, 1986)
24. $CH_4 + OH = CH_3 + H_2O$	1.93E05	2.40	2105	7.94E02	2.84	15251	(Tsang and Hampson, 1986)
25. $CH_4 + O_2 = CH_3 + HO_2$	4.03E13	0.00	56879	5.50E10	0.24	369	(Tsang and Hampson, 1986)
26. $CH_4 + HO_2 = CH_3 + H_2O_2$	1.81E11	0.00	18569	2.66E10	−0.11	−291	(Tsang and Hampson, 1986)
27. $CH_3 + H = CH_2 + H_2$	9.00E13	0.00	15100	1.77E10	0.82	8123	(Glarborg *et al.*, 1986)
28. $CH_3 + O = CH_2O + H$	7.83E13	0.00	0	1.94E16	−0.35	70658	(Tsang and Hampson, 1986)
29. $CH_3 + OH = CH_3O + H$	9.00E14	0.00	15400	5.05E20	−1.14	5526	(Dagaut *et al.*, 1988)
30. $CH_3 + OH = CH_2 + H_2O$	1.50E13	0.00	5000	1.22E11	0.56	13820	(Glarborg *et al.*, 1986)
31. $CH_3 + O_2 = CH_3O + O$	1.99E18	−1.57	29214.	218E21	−2.27	2061	(Tsang and Hampson, 1986)
32. $CH_3 + O_2 = CH_2O + OH$	3.40E11	0.00	8940	1.64E11	0.09	62321	(Sloane, 1989)
33. $CH_3 + HO_2 = CH_3O + OH$	1.99E13	0.00	0	1.13E15	−0.30	24959	(Tsang and Hampson, 1986)
34. $CH_3 + CH_3 = C_2H_4 + H_2$	1.00E16	0.00	32005	2.41E20	−0.72	90016	(Warnatz, 1984a)
35. $CH_3 + CH_3 = C_2H_5 + H$	8.00E15	0.00	26512	4.32E20	−1.04	17799	[See Text]
36. $CH_3 + CH_3(+M) = C_2H_6(+M)$	9.03E16	−1.18	654	1.33E27	−3.09	93300	(Kee *et al.*, 1989b)
Low pressure limit:	3.18E41	−7.03	2763	4.68E51	−8.94	95407	
Troe parameters: a = 6.04E−01 T^* = 6927 T^{**} = 132							
Enhanced third-body efficiencies[d]:							
H_2/2.0/ H_2O/5.0/ CO/2.0/ CH_4/16 CH_3OH/5/							
37. $CH_2O + M = HCO + H + M$	1.20E41	−6.90	96500	1.74E37	−6.32	4949	(Tsang and Hampson, 1986)
38. $CH_2O + H = HCO + H_2$	1.00E14	0.00	4928	1.38E10	0.75	17278	(Norton and Dryer, 1990)
39. $CH_2O + O = HCO + OH$	1.81E13	0.00	3082	1.78E09	0.70	13694	(Tsang and Hampson, 1986)
40. $CH_2O + OH = HCO + H_2O$	3.43E09	1.18	−447	1.95E07	1.6660	27698	(Tsang and Hampson, 1986)
41. $CH_2O + HO_2 = HCO + H_2O_2$	1.00E12	0.00	8000	2.03E11	−0.06	4143	(Sloane, 1989)
42. $CH_2O + CH_3 = HCO + CH_4$	1.00E10	0.50	6000	1.38E10	0.55	20994	(Sloane, 1989)
43. $CH_3O + M = CH_2O + H + M$	3.91E37	−6.65	33246	2.54E34	−5.97	11638	(Tsang and Hampson, 1986)
Enhanced third-body efficiencies[d]:							
H_2/2.5/ H_2O/16.0/ CO/1.9/ CO_2/3.8/ CH_4/16/ CH_3OH/5/							
44. $CH_3O + H = CH_2O + H_2$	1.99E13	0.00	0	1.23E10	0.85	82263	(Tsang and Hampson, 1986)
45. $CH_3O + O = CH_2O + OH$	6.02E12	0.00	0	2.66E09	0.79	80524	(Tsang and Hampson, 1986)
46. $CH_3O + OH = CH_2O + H_2O$	1.81E13	0.00	0	4.62E11	0.59	98055	(Tsang and Hampson, 1986)

TABLE I (continued)

Reaction	Forward rate[b]			Backward rate			Reference
	A	β	E_a	A	β	E_a	
47. $CH_3O + O_2 = CH_2O + HO_2$	6.62E10	0.00	2602	5.61E08	0.39	31027	(Tsang and Hampson, 1986)
48. $CH_3O + HO_2 = CH_2O + H_2O_2$	3.01E11	0.00	0	2.74E11	0.04	66057	(Tsang and Hampson, 1986)
49. $CH_3O + CO = CH_3 + CO_2$	1.57E13	0.00	11797	2.20E14	−0.18	47836	(Tsang and Hampson, 1986)
50. $CH_3O + C_2H_5 = CH_2O + C_2H_6$	2.41E13	0.00	0	4.26E15	−0.19	79755	(Tsang and Hampson, 1986)
51. $CH_3O + C_2H_3 = CH_2O + C_2H_4$	2.41E13	0.00	0	1.11E15	−0.15	87709	(Tsang and Hampson, 1986)
52. $CH_3O + C_2H = CH_2O + C_2H_2$	2.42E13	0.00	0	5.84E14	−0.33	111284	(Tsang and Hampson, 1986)
53. $HCO + M = H + M$	5.12E21	−2.14	20412	1.08E20	−1.63	4424	(Tsang and Hampson, 1986)
Enhanced third-body efficiencies[d]: H_2/2.5/ H_2O/16.0/ CO/1.9/ CH_2/3.8 CH_4/16/ CH_3OH/5/							
54. $HCO + H = CO + H_2$	7.24E13	0.00	0	1.46E12	0.69	87877	(Yetter *et al.*, 1990)
55. $HCO + O = CO + OH$	3.02E13	0.00	0	4.35E11	0.63	86138	(Yetter *et al.*, 1990)
56. $HCO + OH = CO + H_2O$	3.02E13	0.00	0	2.52E13	0.42	103669	(Yetter *et al.*, 1990)
57. $HCO + O_2 = CO + HO_2$	1.42E13	0.00	410	4.20E12	0.22	34450	[See Text]
58. $HCO + HO_2 = CO_2 + OH + H$	3.00E13	0.00	0	5.07E14	0.030	45027	(Norton and Dryer, 1990)
59. $CO + O + M = CO_2 + M$	2.51E13	0.00	−4540	1.34E20	1.21	123757	(Yetter *et al.*, 1990)
Enhanced third-body efficiencies[d]: H_2/2.5/ H_2O/16.0/ CO/1.9/ CO_2/3.8/ CH_4/16/ CH_3OH/5/							
60. $CO + OH = CO_2 + H$	1.50E07	1.30	−765	1.18E14	−0.02	25415	(Yetter *et al.*, 1990)
61. $CO + O_2 = CO_2 + O$	2.51E12	0.00	47690	3.85E16	−0.88	56573	(Yetter *et al.*, 1990)
62. $CO + HO_2 = CO_2 + OH$	5.75E130	0.00	22940	4.59E16	−0.48	83933	(Yetter *et al.*, 1990)
63. $CH + O = CO + H$	5.70E13	0.00	0	1.02E15	0.12	175499	(Glarborg *et al.*, 1986)
64. $CH + OH + HCO + H$	3.00E13	0.00	0	3.73E16	−0.15	89361	(Glarborg *et al.*, 1986)
65. $CH + O_2 = HCO + O$	3.30E13	0.00	0	7.99E13	−0.07	72089	(Glarborg *et al.*, 1986)
66. $CH + CO_2 = HCO + CO$	3.40E12	0.00	690	5.37E08	0.81	63872	(Clarborg *et al.*, 1986)
67. $CH_2 + H = CH + H_2$	3.01E13	0.00	0	5.89E12	0.15	2358	(Tsang and Hampson, 1986)
68. $CH_2 + O = CO + H + H$	1.51E13	0.00	0	5.55E13	0.09	74002	(Tsang and Hampson, 1986)
69. $CH_2 + O = CO\,H_2$	1.51E13	0.00	0	5.29E13	0.27	177857	(Tsang and Hampson, 1986)
70. $CH_2 + OH = CH_2O + H$	3.01E13	0.00	0	5.31E19	−1.11	79367	(Tsang and Hampson, 1986)
71. $CH_2 + OH = CH + H_2O$	4.50E13	0.00	3000	3.63E14	−0.11	21149	(Glarborg *et al.*, 1986)
72. $CH_2 + O_2 = CO_2 + H + H$	1.60E12	0.00	1000	9.01E16	−0.79	83909	(Glarborg *et al.*, 1986)
73. $CH_2 + O_2 = CH_2O + O$	2.00E13	0.00	9000	6.87E16	−0.67	71090	(Glarborg *et al.*, 1986
74. $CH_2 + O_2 = CO_2 + H_2$	6.90E11	0.00	500	3.71E16	−0.62	187263	(Glarborg *et al.*, 1986)

75.	$CH_2 + O_2 = CO + H_2O$	1.90E10	0.00	1000	5.35E09	0.44	175377	(Glarborg *et al.*, 1986)
76.	$CH_2 + O_2 = CO + OH + H$	8.60E10	0.00	500	6.15E08	0.53	56231	(Glarborg *et al.*, 1986)
77.	$CH_2 + HO_2 = CH_2O + OH$	3.01E13	0.00	0	5.38E15	−0.27	114192	(Tsang and Hampson, 1986)
78.	$CH_2 + H_2O_2 = CH_2O + OH$	3.01E13	0.00	0	5.91E15	−0.31	48135	(Tsang and Hampson, 1986)
79.	$CH_2 + CO_2 = CH_2O + CO$	1.10E11	0.00	1000	2.47E10	0.21	54187	(Glarborg *et al.*, 1986)
80.	$CH_2 + CH_2O = CH_3 + HCO$	1.20E12	0.00	0	8.41E11	−0.07	19322	(Tsang and Hampson, 1986)
81.	$CH_2 + HCO = CH_3 + CO$	1.81E13	0.0	0	1.86E15	−0.14	94846	(Tsang and Hampson, 1986)
82.	$CH_2 + CH_3 = C_2H_4 + H$	1.81E13	0.0	0	2.21E21	−1.55	64997	(Tsang and Hampson, 1986)
83.	$CH_2 + CH_2 = C_2H_2 + H_2$	4.00E13	0.00	0	2.88E20	−1.26	131621	(Miller *et al.*, 1982)
84.	$C_2H_6 + H = C_2H_5 + H_2$	5.54E02	3.50	5164	1.94E−03	4.55	7670	(Tsang and Hampson, 1986)
85.	$C_2H_6 + O = C_2H_5 + OH$	1.20E12	0.60	7308	2.99E06	1.59	8074	(Tsang and Hampson, 1986)
86.	$C_2H_6 + OH = C_2H_5 + H_2O$	8.85E09	1.04	1813	1.28E06	1.82	20113	(Tsang and Hampson, 1986)
87.	$C_2H_6 + O_2 = C_2H_5 + HO_2$	4.03E13	0.00	50842	1.93E09	0.59	−512	(Tsang and Hampson, 1986)
88.	$C_2H_6 + HO_2 = C_2H_5 + H_2O_2$	2.95E11	0.00	14935	1.52E09	0.24	1230	(Tsang and Hampson, 1986)
89.	$C_2H_5(+M) = C_2H_4 + H(+M)$[c]	4.90E09	1.19	37182	2.29E09	1.33	36	(Tsang and Hampson, 1986)
	Low pressure limit:	2.39E55	−11.4	53042	1.12E55	−11.3	15888	
	Enhanced third-body efficiencies[d]: H_2/2.5/ H_2O/16.0/ CO/1.9/ CO_2/3.8/ CH_4/16/ CH_3OH/5/							
90.	$C_2H_5 + H = C_2H_4 + H_2$	1.81E12	0.00	0	8.08E11	0.32	66726	(Tsang and Hampson, 1986)
91.	$C_2H_5 + O = C_2H_4 + OH$	5.00E13	0.00	0	1.59E13	0.26	64988	(Hennessy *et al.*, 1986)
92.	$C_2H_5 + O = CH_3HCO + H$	9.64E13	0.00	0	3.26E17	−0.65	74956	(Tsang and Hampson, 1986)
93.	$C_2H_5 + OH = C_2H_4 + H_2O$	2.41E13	0.00	0	4.44E14	0.05	82519	(Tsang and Hampson, 1986)
94.	$C_2H_5 + O_2 = C_2H_4 + HO_2$	8.43E11	0.00	3875	5.15E12	−0.15	16763	(Tsang and Hampson, 1986)
95.	$C_2H_5 + CH_4 = C_2H_6 + CH_3$	8.62E−02	4.14	12555	2.45E00	3.80	7395	(Tsang and Hampson, 1986)
96.	$C_2H_4 + M = C_2H_2 + H_2 + M$	2.60E17	0.00	792978	3.16E12	0.93	35057	(Warnatz, 1984a)
	Enhanced third-body efficiencies[d]: H_2/2.5/ H_2O/16.0/ CO/1.9/ CO_2/3.8/ CH_4/16/ CH_3OH/5/							
97.	$C_2H_4 + M = C_2H_3 + H + M$	2.60R17	0.00	96494	3.66E12	0.83	−12855	(Warnatz, 1984a)
	Enhanced third-body efficiencies[d]: H_2/2.5/ H_2O/16.0/ CO/1.9/ CO_2/3.8/ CH_4/16/ CH_3OH/5/							
98.	$C_2H_4 + H = C_2H_3 + H_2$	1.32E06	2.53	12234	1.77E01	3.53	6782	(Tsang and Hampson, 1986)
99.	$C_2H_4 + O = CH_3 + HCO$	1.32E08	1.55	427	1.87E02	2.68	25410	(Tsang and Hampson, 1986)
100.	$C_2H_4 + O = CH_2O + CH_2$	4.00E12	0.00	5000	8.10E06	1.20	10659	(Dagaut *et al.*, 1988)
101.	$C_2H_4 + OH = C_2H_3 + H_2O$	1.57E04	2.75	4171	8.70E00	3.49	14516	(Tsang and Hampson, 1986)
102.	$C_2H_4 + OH = CH_3 + CH_2O$	1.50E12	0.00	960	2.16E10	0.43	15329	(Dagaut *et al.*, 1988)
103.	$C_2H_4 + O_2 = C_2H_3 + HO_2$	4.22E13	0.00	57594	7.76E09	0.54	−1717	(Tsang and Hampson, 1986)
104.	$C_2H_4 + CO = C_2H_3 + HCO$	1.51E14	0.00	90562	1.00E11	0.32	−2806	(Tsang and Hampson, 1986)

TABLE I (continued)

Reaction	Forward rate[b] A	β	E_a	Backward rate A	β	E_a	Reference
105. $C_2H_3(+M) = C_2H_2 + H(+M)$[c]	1.60E14	0.00	37977	1.45E14	−0.07	−797	(Warnatz, 1984a)
Low pressure limit:	3.00E15	0.00	32006	2.71E15	−0.07	−6765	
Enhanced third-body efficiencies[d]: H_2/2.5/ H_2O/16.0/ CO/1.9/ CO_2/3.8/ CH_4/16/ CH_3OH/5/							
106. $C_2H_3 + H = C_2H_2 + H_2$	4.00E13	0.00	0	3.45E13	0.11	65100	(Kee *et al.*, 1989b)
107. $C_2H_3 + O = CH_2CO + H$	9.64E13	0.00	0	2.31E17	−0.62	87875	(Tsang and Hampson, 1986)
108. $C_2H_3 + OH = H_2O + C_2H_2$	3.01E13	0.00	0	1.07E15	−0.16	80892	(Tsang and Hampson, 1986)
109. $C_2H_3 + O_2 = C_2H_2 + HO_2$	1.20E11	0.00	0	1.42E12	−0.36	11263	(Tsang and Hampson, 1986)
110. $C_2H_3 + O_2 = CH_2O + HCO$	0.80E12	0.00	−350	0.57E11	0.27	85204	[See Text]
111. $C_2H_3 + C_2H_3 = C_2H_4 + C_2H_2$	1.49E14	0.00	−2614	4.95E18	−0.69	69560	(Sloane, 1989)
112. $C_2H_2 = C_2H + H$	1.80E41	−7.76	137510	4.82E36	−6.87	4565	(Tsang and Hampson, 1986)
113. $C_2H_2 + H = C_2H + H_2$	6.02E13	0.00	22243	1.54E09	1.07	−6790	(Tsang and Hampson, 1986)
114. $C_2H_2 + O = CH_2 + CO$	1.75E13	0.00	3178	8.53E06	1.52	49412	(Tsang and Hampson, 1986)
115. $C_2H_2 + O = HCCO + H$	4.3-E14	0.00	12110	6.63E13	0.05	30522	(Warnatz, 1984a)
116. $C_2H_2 + OH = C_2H + H_2O$	1.45E04	2.68	12035	1.53E01	3.48	−1200	(Tsang and Hampson, 1986)
117. $C_2H_2 + OH = CH_2CO + H$	3.00E12	0.00	1099	1.17E16	−0.67	25613	(Warnatz, 1984b)
118. $C_2H_2 + O_2 = C_2H + HO_2$	1.20E13	0.00	74475	4.19E09	0.61	−8420	(Tsang and Hampson, 1986)
119. $C_2H + O = CH + CO$	1.81E13	0.00	0	6.77E10	0.61	77615	(Tsang and Hampson, 1986)
120. $C_2H + O_2 = CO + HCO$	2.41E12	0.00	0	2.18E10	0.54	149704	(Tsang and Hampson, 1986)
121. $CH_2CO(+M) = CH_2 + CO(+M)$[c]	3.00E14	0.00	70937	5.52E04	2.08	−9492	(Warnatz, 1984a)
Low pressure limit:	3.60E15	0.00	59235	6.62E05	2.08	−21188	
Enhanced third-body efficiencies[d]: H_2/2.5 H_2O/16.0/ CO/1.9/ CO_2/3.8/ CH_4/16/ CH_3OH/5/							
122. $CH_2CO + H = CH_3 + CO$	1.10E13	0.00	3430	9.79E06	1.43	33859	(Glarborg *et al.*, 1986)
123. $CH_2CO + H = HCCO + H_2$	7.50E13	0.00	8000	4.14E09	0.78	3639	(Glarborg *et al.*, 1986)
124. $CH_2CO + O = HCO + HCO$	2.00E13	0.00	2293	3.01E07	1.15	27856	(Warnatz, 1984a)
125. $CH_2CO + O = CH_2O + CO$	2.00E13	0.00	0	4.41E09	1.08	101089	(Glarborg *et al.*, 1986)
126. $CH_2CO + O = HCCO + OH$	5.00E13	0.00	8000	1.98E09	0.72	1900	(Glarborg *et al.*, 1986)
127. $CH_2CO + OH = CH_2O + HCO$	2.80E13	0.00	0	4.29E11	0.45	14951	(Glarborg *et al.*, 1986)
128. $CH_2CO + OH = HCCO + H_2O$	7.50E12	0.00	3000	1.72E10	0.51	14434	(Glarborg *et al.*, 1986)
129. $HCCO + H = CH_2 + CO$	1.10E14	0.00	0	3.48E08	1.48	27817	(Glarborg *et al.*, 1986)
130. $HCCO + O = CO + CO + H$	1.10E14	0.00	0	1.28E09	1.57	101820	(Glarborg *et al.*, 1986)

131.	$HCCO + OH = HCO + CO + H$	1.00E13	0.00	0	8.07E09	0.94	15682	(Glarborg *et al.*, 1986)
132.	$HCCO + O_2 = CO + CO + OH$	1.50E12	0.00	2500	3.39E04	2.01	87046	(Glarborg *et al.*, 1986)
133.	$HCCO + CH_2 = C_2H + CH_2O$	1.00E13	0.00	2000	2.08E15	−0.15	32187	(Glarborg *et al.*, 1986)
134.	$HCCO + CH_2 = C_2H_2 + CO$	3.00E13	0.00	0	7.91E14	0.11	94338	(Glarborg *et al.*, 1986)
135.	$HCCO + HCCO = C_2H_2 + CO + CO$	1.00E13	0.00	0	7.54E08	1.52	83401	(Glarborg *et al.*, 1986)
136.	$CH_3HCO = CH_3 + HCO$	2.00E15	0.00	79058	3.92E05	1.92	−8082	(Warnatz, 1984a)
137.	$CH_3HCO + H = CH_3 + CO + H2$	4.00E13	0.00	4204	1.59E02	2.61	4978	(Warnatz, 1984a)
138.	$CH_3HCO + O = CH_3CO + OH$	5.00E12	0.00	1791	2.98E08	0.86	16541	(Warnatz, 1984a)
139.	$CH_3HCO + OH = CH_3CO + H2O$	1.00E13	0.00	0	3.45E10	0.65	32282	(Warnatz, 1984a)
140.	$CH_3CO + M = CH_3 + CO + M$	1.20E15	0.00	12516	5.69E07	1.69	−3204	(Warnatz, 1984a)
141.	$CH_3CO + H = CH_3 + HCO$	9.64E13	0.00	0	2.16E08	1.18	264	(Tsang and Hampson, 1986)
142.	$CH_3CO + O = CH_3 + CO_2$	9.64E12	0.00	0	2.45E12	0.49	112581	(Tsang and Hampson, 1986)
143.	$CH_3CO + OH = CH_2CO + H_2O$	1.20E13	0.00	0	2.52E13	0.17	73503	(Tsang and Hampson, 1986)
144.	$CH_3CO + OH = CH_3 + CO + OH$	3.01E13	0.00	0	1.43E06	1.69	−15713	(Tsang and Hampson, 1986)
145.	$CH_3CO + H_2 = CH_3HCO + H$	4.09E06	1.82	17600	4.89E10	0.91	1102	(Tsang and Hampson, 1986)
146.	$CH_3CO + HO_2 = CH_3 + CO_2 + OH$	3.01E13	0.00	0	1.14E09	1.21	45291	(Tsang and Hampson, 1986)
147.	$CH_3CO + H_2O_2 = CH_3HCO + HO_2$	1.81E11	0.00	8222	1.47E12	−0.11	7934	(Tsang and Hampson, 1986)
148.	$CH_3CO + HCO = CH_3HCO + CO$	9.03E12	0.00	0	2.18E15	−0.23	71387	(Tsang and Hampson, 1986)
149.	$CH_3CO + CH_4 = CH_3HCO + CH_3$	2.17E03	2.88	21449	2.59E03	2.67	2304	(Tsang and Hampson, 1986)
150.	$CH_3CO + C_2H_6 = C_2H_5 + CH_3HCO$	1.81E04	2.75	17517	7.58E02	2.88	3527	(Tsang and Hampson, 1986)
151.	$CH_3CO + CH_2O = CH_3HCO + HCO$	1.81E11	0.00	12909	2.99E11	−0.16	8765	(Tsang and Hampson, 1986)
152.	$CH_3OH(+M) = CH_3 + OH(+M)^c$	1.90E16	0.00	91780	1.24E09	1.31	−2767	(Tsang, 1987, Fit)
	Low pressure limit:	8.86E46	−7.93	102641	5.77E39	−6.62	8088	
153.	$CH_3OH(+M) = CH_2OH + H(+M)^c$	1.54E16	0.00	96844	6.01E12	0.35	−923	(Tsang, 1987, Fit)
	Low pressure limit:	7.20E46	−7.93	107705	2.81E43	−7.58	9932	
154.	$CH_3OH + H = CH_2OH + H_2$	3.20E13	0.00	6095	1.19E10	0.52	12228	(Norton and Dryer, 1990)
155.	$CH_3OH + H = CH_3O + H_2$	8.00E12	0.00	6095	2.79E11	0.35	5579	(Norton and Dryer, 1990)
156.	$CH_3OH + O = CH_2OH + OH$	3.88E05	2.50	3080	1.03E02	2.97	7475	(Norton and Dryer, 1990)
157.	$CH_3OH + OH = CH_2OH + H_2O$	1.50E13	0.00	5960	2.30E11	0.26	27885	(Bowman, 1975, See Text)
158.	$CH_3OH + OH = CH_3O + H_2O$	1.50E13	0.00	5960	2.16E13	0.080	21237	(Bowman, 1975, See Text)
159.	$CH_3OH + O_2 = CH_2OH + HO_2$	2.05E13	0.00	44717	1.04E11	0.06	−3006	(Norton and Dryer, 1990)
160.	$CH_3OH + HO_2 = CH_2OH + H_2O_2$	3.98E13	0.00	19400	2.18E13	−0.29	9321	(Norton and Dryer, 1990)
161.	$CH_3OH + CH_3 = CH_2OH + CH_4$	3.19E01	3.17	7172	1.19E02	2.99	15949	(Norton and Dryer, 1990)
162.	$CH_3OH + CH_3 = CH_3O + CH_4$	1.45E01	3.10	6935	5.08E03	2.74	9064	(Norton and Dryer, 1990)
163.	$CH_2OH + M = CH_2O + H + M$	2.43E28	−4.00	31887	1.48E27	−3.50	3631	(Tsang, 1987, Fit)
164.	$CH_2OH + H = CH_2O + H_2$	3.00E13	0.00	0	1.74E12	0.67	75614	(Norton and Dryer, 1990)
165.	$CH_2OH + O_2 = CH_2O + HO_2$	2.41E14	0.00	5000	1.92E14	0.21	26775	(Norton and Dryer, 1990)

TABLE I (continued)

Reaction	Forward rate[b]			Backward rate			Reference
	A	β	E_a	A	β	E_a	
166. $CH_2OH + HO_2 = CH_2O + H_2O_2$	1.20E13	0.00	0	1.03E15	−0.13	59409	(Norton and Dryer, 1990)
167. $CH_2OH + HCO = CH_3OH + CO$	1.20E14	0.00	0	6.52E15	0.16	81741	(Norton and Dryer, 1990)
168. $CH_2OH + CH_3 = C_2H_5 + OH$	1.37E14	−0.41	6589	1.24E15	−0.48	1103	(Norton and Dryer, 1990)
169. $CH_2OH + CH_3OP = HCO + CH_3OH$	5.54E03	2.81	5862	2.06E03	3.04	12075	(Norton and Dryer, 1990)
170. $CH_2OH + CH_2OH = CH_3OH + CH_2O$	1.20E13	0.00	0	1.87E15	0.15	69478	(Norton and Dryer, 1990)
171. $CH_2OH + H = CH_3 + OH$	2.39E02	3.35	−2071	3.99E−02	4.31	248	(Grotheer and Kelm, 1989)

[a] Reaction mechanism rate coefficients in the form $k_f = AT^{\beta} \exp(-E_a/RT)$ (units are moles, cubic centimeters, seconds, Kelvins and calories/mole).

[b] Forward rate taken from the reported reference.

[c] Backward rate calculated from forward by equilibrium using the CHEMKIN (Kee *et al.*, 1987) thermodynamic data.

[d] Only species with non-unity collision efficiency are specified.

[e] Fall-off reaction in the Lindemann form given the high and low pressure limits.

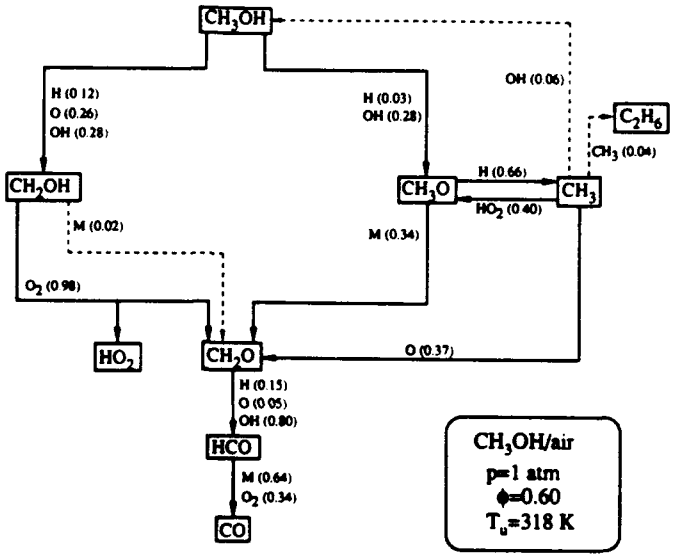

FIGURE 4 Species consumption path analysis for lean methanol/air flame ($\phi = 0.6$) at $T_u = 318$ K and $p = 1$ atm.

Furthermore the S_u^0's for methanol/air mixtures at $T_u = 298$ K are slightly higher than those of methane/air, and in general are comparable to other paraffin/air mixtures at the same initial conditions.

Figure 2 shows the numerically calculated results and their close agreements with the experimental data. The kinetic scheme, listed in Table I, includes 30 species and 171 reversible reactions for the C_1, C_2, and CH_3OH submechanisms. Its compilation was conducted iteratively since the validity of certain reactions could not be assessed by using the flame speed data alone. For the C_1 and C_2 submechanisms, the starting point was the mechanism compiled by Egolfopoulos *et al.* (1990, 1991) (reactions R1 through R151) which closely predicts the laminar flame speeds of mixtures of CH_4 and the C_2-hydrocarbons with O_2 and N_2 for various stoichiometries and pressures. For the CH_3OH submechanism a combination of the latest information of Norton and Dryer (1989, 1990) was used on methanol oxidation and pyrolysis (reactions R152 through R171). For each reaction in Table I the forward rate is reported along with its source; the code determines the backward rate through thermodynamic equilibrium using the thermnodynamic data of Kee *et al.* (1987). The fitted backward rates are also reported in Table I so that the accurate use of the present scheme by others is facilitated.

In order to utilize the laminar flame speed comparisons for the validation of the kinetic scheme, it is important to identify the main species consumption paths in methanol flames and conduct sensitivity analysis (Kee *et al.*, 1985; Grcar *et al.*, 1986) by determining the influence of all reaction rates on the laminar mass burning rate $\dot{m}'' = \rho_u S_u^0$, where ρ_u is the density of the unburned mixture.

The species consumption paths are shown in Figures 4, 5, and 6 for lean, stoichiometric, and rich flames respectively. These paths were determined by integrating all reactions through the flame and determining the fraction of each species consumed by a specific reaction; this fraction is indicated next to each species. From such a study the following observations can be made:

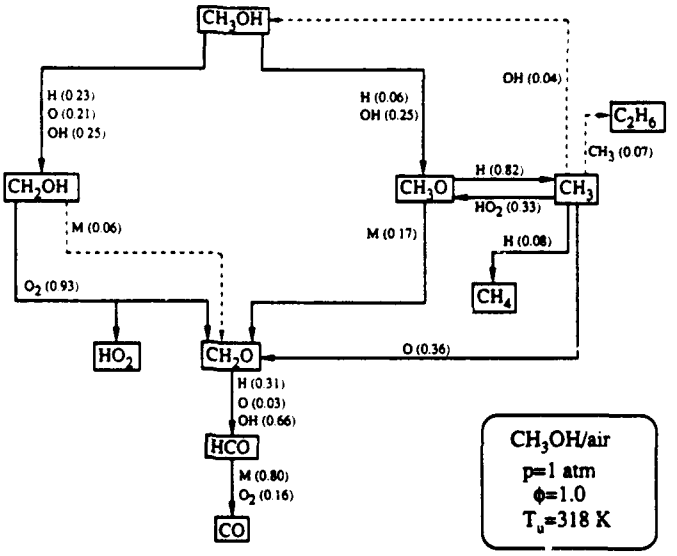

FIGURE 5 Species consumption path analysis for stoichiometric methanol/air flame (ϕ = 1.0) at T_u = 318 K and p = 1 atm.

(1) CH_3OH: It is attacked by H, O, OH, and HO_2. About 70 to 75% is converted to the hydroxymethyl radical (CH_2OH), while only 25 to 30% is converted to the methoxy radical (CH_3O). Even at this stage the very different nature of methanol chemistry is obvious as compared to methane for which the methyl radical (CH_3) is produced after the initial fuel reactions. For mechanol flames it is clear that understanding of the kinetic behavior of the oxygenated compounds, CH_2OH and CH_3O,

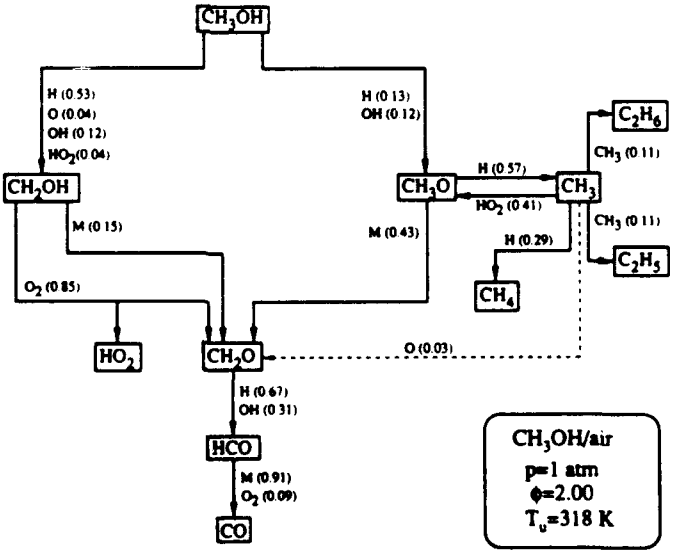

FIGURE 6 Species consumption path analysis for rich methanol/air flame (ϕ = 2.0) at T_u = 318 K and p = 1 atm.

is crucial to the compilation of a reliable kinetic scheme, while the knowledge of the CH_3 chemistry is not as important. Among the various radicals attacking CH_3OH, the OH consumes almost 50–60% for lean and stoichiometric flames for which OH is available, and decreases to about 25% for rich flames due to reduced concentrations of OH. The attack by H is less important for lean and stoichiometric flames than for rich flames where it contributes to almost 70% of the fuel consumption. The reaction with O also becomes progressively less important as the mixture becomes richer due to the decreased O concentration.

(2) CH_2OH: This is the main product of the initial fuel reactions, and for all stoichiometries there are only two consumption paths. The most important is the reaction with O_2, with the thermal decomposition route becoming somewhat important for rich flames due to the reduced supply of O_2. The reaction of CH_2OH with O_2 produces CH_2O as well as HO_2. Generation of the latter indicates an additional difference between methane and methanol in that HO_2 can also be produced in substantial amounts by means other than reactions R9 and R10 ($H + O_2 + M = HO_2 + M$). Therefore, reactions of HO_2 are expected to be of increased importance as compared to those in hydrocarbon flames.

(3) CH_3O: Its main consumption paths are very different from those of CH_2OH, indicating the importance of considering both CH_2OH and CH_3O in recent studies. The methoxy radicals either react with H or thermally decompose. Thermal decomposition leads to CH_2O and it is more important for lean and rich flames as compared to the stoichiometric flame. The reaction with H is the main source of CH_3 radicals and is more important for stoichiometric flames due to the abundance in H. For significantly off-stoichiometric mixtures, the H concentration decreases, resulting in an increased importance of the thermal decomposition route. It is interesting to note that, in contrast to CH_2OH, the reaction with O_2 does not appear to be important.

(4) CH_3: It exists in small concentrations because it is produced by the partial consumption of CH_3O whose concentration is significantly lower than that of CH_2OH. For lean and stoichiometric flames it partially reacts with O leading to CH_2O; for all stoichiometries 30–40% of the CH_3 reacts with HO_2 leading to CH_3O. The reaction with HO_2 is important due to the increased amount of HO_2 in methanol flames. The reactions with H and CH_3, which respectively lead to CH_4 and C_2-hydrocarbons, become more important for rich flames, although the rates of these consumption paths are lower than those in methane flames.

(5) CH_2O: From the species consumption diagrams shown in Figures 4, 5, and 6, it is seen that for all stoichiometries approximately one mole of CH_2O is produced from one mole of CH_3OH. In contrast, in methane flames the direct production of CH_2 and HCO radicals as well as C_2 species provides alternate paths, as shown in Figure 7 where the species consumption paths for atmospheric, stoichiometric CH_4/air flames are illustrated.

A comparison between methanol and methane combustion with regard to the production of selected species is shown in Figure 8. The reported data represent the ratio between the total number of moles of each species present throughout a methanol/air flame and the corresponding number of moles for a methane/air flame at $p = 1$ atm and $\phi = 1$ conditions. Results show that the CH_2O and HO_2 concentrations present in a methanol flame are respectively 15 and 4 times higher than those in the methane flame. The concentrations of the C_2-hydrocarbons present in methanol flames are, however, only fractions of those of the methane flame. These results quantitatively demonstrate the lower propensity of methanol to soot, due to the lower C_2-hydrocarbon production, and at the same time its higher propensity for CH_2O production.

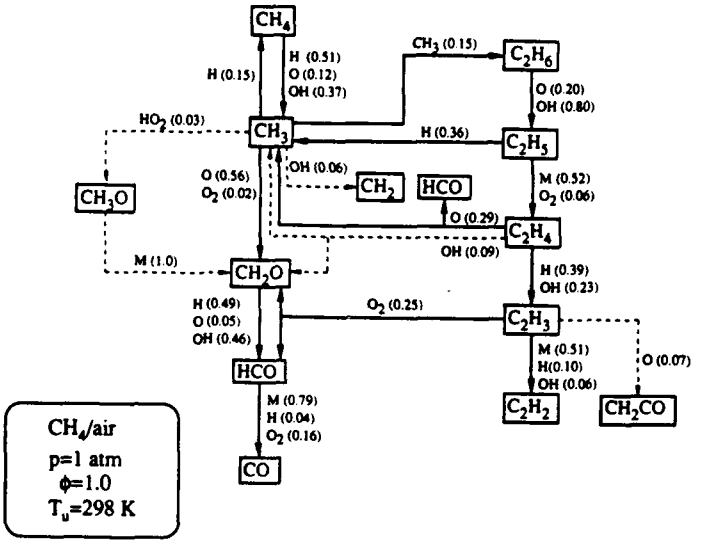

FIGURE 7 Species consumption path analysis for stoichiometric (ϕ = 1.0) methane/air flame at T_u = 298 K and p = 1 atm.

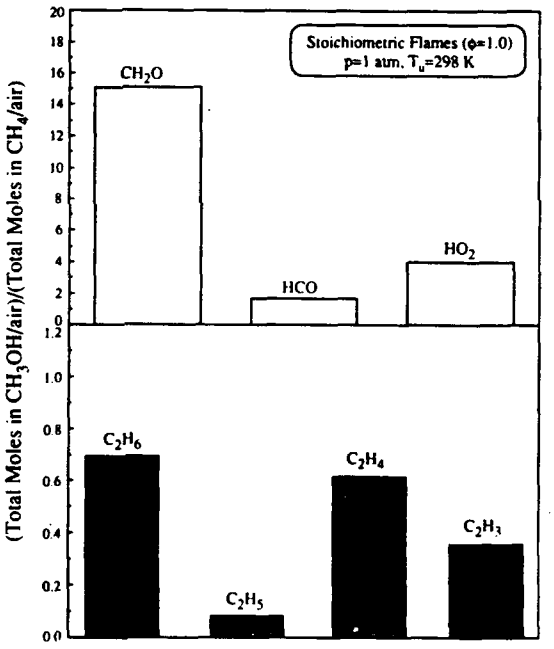

FIGURE 8 Ratio of the total number of moles of selected species present in a stoichiometric methanol/air flame (ϕ = 1.0) at T_u = 298 K and p = 1 atm over the corresponding number for stoichiometric methane/air (ϕ = 1.0) flame at the same conditions. Top: CH_2O, HCO, and HO_2. Bottom: C_2-hydrocarbons.

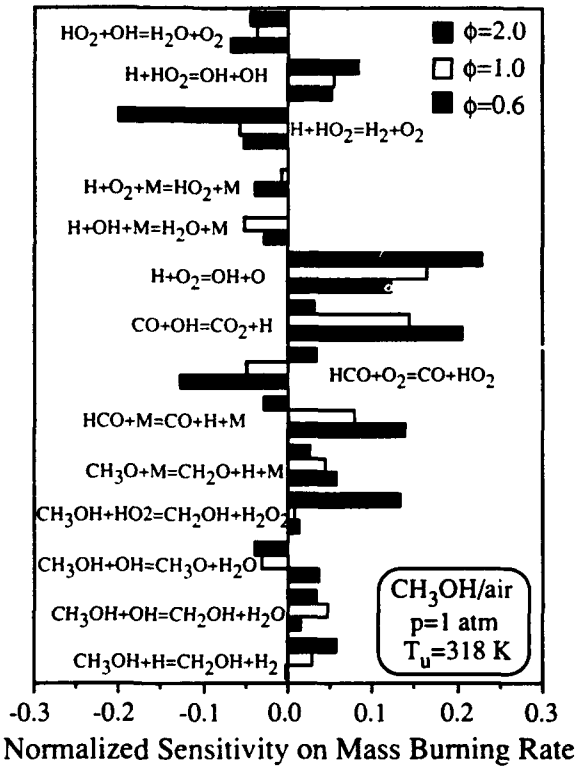

FIGURE 9 Normalized first order sensitivity coefficients of the most important reactions on the mass burning rate of lean, stoichiometric, and rich methanol/air flames at T_u = 318 K and p = 1 atm.

The first order normalized sensitivity coefficients (Kee *et al.*, 1985; Grcar *et al.*, 1986) of selected reactions on the mass burning rate, m^0, of lean, stoichiometric, and rich flames are shown in Figure 9. A "shift" of the importance of certain reactions can be seen as the stoichiometry changes from lean to rich. Based on the results of Figures 4, 5, 6 and 9, the role of the key reactions on the overall rate progress can now be assessed:

(1) Reaction R1 ($H + O_2 = OH + O$): It has high positive sensitivity on m^0 for all flames due to its chain branching nature, and is the most dominant reaction for rich flames. Similar behavior exists for hydrocarbons (Egolfopoulos *et al.*, 1990, 1991).

(2) Reactions R9 ($H + O_2 + M = HO_2 + M$, $M \neq H_2O$) and R10 ($H + O_2 + H_2O = HO_2 + H_2O$): They compete directly with R1 for the same radicals, producing the relatively inactive HO_2 and hence providing significant termination paths for lean flames. For rich flames, however, the termination is minimal.

(3) Reaction R60 ($CO + OH = CO_2 + H$): This is the main CO oxidation reaction, producing heat and H radicals. For lean flames its positive sensitivity on m^0 dominates even that of R1 because there is enough O_2 to oxidize CO to CO_2. Its importance, however, is gradually diminished as the stoichiometry becomes richer because there is not sufficient O_2 to oxidize CO. As a result, CO assumes the role of an abundant "final product" species and its rate of oxidation is no longer a controlling factor.

(4) Reactions R53 ($HCO + M = CO + H + M$) and R57 ($HCO + O_2 = CO + HO_2$): The thermal decomposition reaction R53 has high positive sensitivity

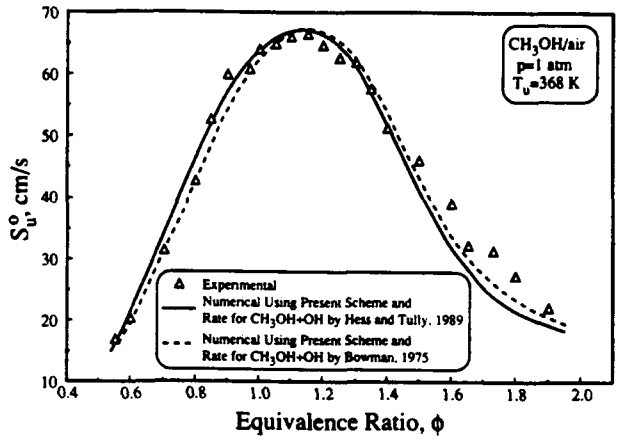

FIGURE 10 Comparison between the experimentally determined $S_u^0(\phi)$ of methanol/air flame at T_u = 368 K and numerical calculations using the present scheme with the rate for reaction $CH_3OH + OH$ taken from Hess and Tully (1989) and Bowman (1975).

on m^0 for lean flames and provides termination for rich flames. Reaction R57 is an alternate path for the consumption of the formyl radicals and its sensitivity behaves exactly opposite to that of R53. For lean flames its rate is favored over R53 due to the excess O_2 present, and provides significant termination because it produces HO_2 which is less essential for the propagation of lean flames as compared to H. For rich flames, which are sensitive to all potential sources of OH, R57 favors propagation by producing additional HO_2 which can either branch to 2OH by reacting with H, or attack the fuel molecule through R160 ($CH_3OH + HO_2 = CH_2OH + H_2O_2$) which produces H_2O_2 and eventually 2OH through decomposition. As a result its direct competitor R53, which produces the less essential CO and H on the rich side, has a negative effect on m^0. For laminar flame comparisons the rate of R57 was assumed to be twice that of Timonen *et al.* (1988), in which the uncertainty factor is stated as 5. This modification was needed in order to obtain closer agreements for the laminar flame speeds of lean mixtures, which were initially overpredicted by 2–3 cm/s. (5) Reactions R157 ($CH_3OH + OH = CH_2OH + H_2O$) and R158 ($CH_3OH + OH = CH_3O + H_2O$): For lean flames, propagation is favored by both reactions but the associated sensitivity is small because their progress is fast, leading to an almost 60% fuel consumption. For rich flames, however, this amount drops to about 25% and m^0 becomes more sensitive to these rates, with the CH_2OH showing a positive sensitivity while the competing CH_3O path has a negative effect. The sign reversal of the sensitivity of the CH_3O path for stoichiometric and rich concentrations is due to the fact that through this path CH_3, CH_4, and C_2-hydrocarbons can be formed instead of CH_2O. This can retard propagation as compared to the CH_2OH path which leads directly to the more reactive CH_2O. The rates of these reactions were obtained from two sources. The first was from Hess and Tully (1989) which was also used by Norton and Dryer (1990). The second, included in Table I, was from Bowman (1975) with a rate which is lower than that of Hess and Tully by a factor of 3.2 to 3.5 for $T > 1000$ K. Figure 10 shows a small difference in the calculated flame speeds using these two rates. Comparisons with the turbulent flow reactor oxidation data to be discussed subsequently, however, demonstrate that significant differences exist in the calculated species profiles and a rate which follows that of Bowman rate yields substantially closer agreement.

(6) Reactions R154 ($CH_3OH + H = CH_2OH + H_2$) and R155 ($CH_3OH + H = CH_3O + H_2$): They are important for rich flames with the CH_2OH path favoring and the CH_3O path retarding propagation, for reasons similar to R157 and R158 respectively.

(7) Reaction R160 ($CH_3OH + HO_2 = CH_2OH + H_2O_2$): It appears to have a significant positive effect on the propagation of rich mixtures. Although fuel consumption by this reaction is small, approximately 4%, its sensitivity is high because it simultaneously produces two species whose subsequent reactions favor propagation. That is, most CH_2OH reactions have positive sensitivity on m^0 while H_2O_2 can also branch to 2OH which is crucial for rich flames. This demonstrates that both sensitivity and species consumption path analyses are needed for accurate assessment of a mechanism.

(8) Reactions R163 ($CH_2OH + M = CH_2O + H + M$) and R43 ($CH_3O + M = CH_2O + H + M$): Reaction R163 does not have a significant effect on propagation due to the increased CH_2OH consumption through R165 ($CH_2OH + O_2 = CH_2O + HO_2$). The reported rate is an appropriately fitted one reported by Tsang (1987). Reaction R43 has a positive effect on propagation for all stoichiometries but its importance decreases for richer flames. The rate used for R43 is the one reported by Tsang and Hampson (1986). These two rates are not well established and their uncertainties have been discussed by Grotheer and Kelm (1989).

(9) HO_2 Reactions: Due to the increased production of HO_2, a number of reactions are shown to be important for both lean and rich flames. Reaction R12 ($HO_2 + H = OH + OH$) leading to 2OH significantly favors propagation for all concentrations and its direct competitor R11 ($HO_2 + H = H_2 + O_2$), leading to the stable species H_2 and O_2, provides significant termination. In particular, for rich flames R11 is the dominant termination path. Furthermore, reactions R14 ($HO_2 + OH = H_2O + O_2$) and R15 ($HO_2 + HO_2 = H_2O_2 + O_2$) have a noticeable effect on propagation as well as the H_2O_2 decomposition reaction R16 ($H_2O_2 + M = OH + OH + M$).

During compilation of the present scheme, calculations were also conducted to assure that the C_1 and C_2 submechanisms (reactions R1 through R151) predict the previously reported flame speed data of mixtures of CH_4 and the C_2-hydrocarbons with air (Egolfopoulos *et al.*, 1989; Egolfopoulos *et al.*, 1990, 1991). Since the thermodynamic data of Kee *et al.* (1987) were used instead of the data of Gordon and McBride (1971), it was necessary to modify the forward rate of reaction R35 ($CH_3 + CH_3 = C_2H_5 + H$) which was shown (Egolfopoulos *et al.*, 1990, 1991) to be crucial for ethane flames. Specifically, it was shown that the backward rate of R35 is an important termination path for ethane flames and that in order to closely predict the experimentally determined ethane/air flame speeds a much faster rate was needed than those reported in the literature. Moreover, it was found that the two main sources of thermodynamic data (Gordon and McBride, 1971; Kee *et al.*, 1987) result in very different equilibrium constants for R35. Values obtained from Kee *et al.* (1987) are 10 times higher than values obtained by using the data of Gordon and McBride (1971) in the temperature range of 1000 and 2500 K. In previous modeling (Egolfopoulos *et al.*, 1990, 1991) the forward rate of Roth and Just (1985) and the low equilibrium constant of Gordon and McBride (1971) were used, so that the backward rate was sufficiently high to assure agreements with the experimental flame speed data. In the present investigation, by adopting the widely accepted data of Kee *et al.* (1987), a forward rate 10 times higher was used for R35. In order to achieve closer agreement for the laminar flame speeds of C_2H_4/mixtures, the rate of Kee *et al.* (1989b) for the reaction

TABLE II

C_3 kinetic scheme used for the determination of the laminar flame speeds of C_2-Hydrocarbons[a]

Reaction	Forward rate[b]			Backward rate[c]			Reference
	A	β	E_a	A	β	E_a	
172. $C_3H_8 = CH_3 + C_2H_5$	1.70E16	0.00	84840	1.75E+04	2.38	−5170	(Pitz and Westbrook, 1986)
173. $C_3H_8 + H = H_2 + i\text{-}C_3H_7$	8.71E06	2.00	5000	1.93E+04	2.75	12259	(Pitz and Westbrook, 1986)
174. $C_3H_8 + H = H_2 + n\text{-}C_3H_7$	5.62E07	2.00	7700	1.11E+04	2.81	10503	(Pitz and Westbrook, 1986)
175. $C_3H_8 + O = i\text{-}C_3H_7 + OH$	2.82E13	0.00	5200	4.45E+10	0.69	10720	(Pitz and Westbrook, 1986)
176. $C_3H_8 + O = n\text{-}C_3H_7 + OH$	1.12E14	0.00	7850	1.57E+10	0.75	8914	(Pitz and Westbrook, 1986)
177. $C_3H_8 + OH = i\text{-}C_3H_7 + H_2O$	4.79E08	1.40	850	4.38E+07	1.89	23904	(Pitz and Westbrook, 1986)
178. $C_3H_8 + OH = n\text{-}C_3H_7 + H_2O$	5.75E08	1.40	850	4.67E+06	1.94	19449	(Pitz and Westbrook, 1986)
179. $C_3H_8 + O_2 = i\text{-}C_3H_7 + HO_2$	3.98E13	0.00	47500	1.21E+12	0.29	901	(Pitz and Westbrook, 1986)
180. $C_3H_8 + n\text{-}C_3H_7 + HO_2$	3.98E13	0.00	47500	1.07E+11	0.34	−3554	(Pitz and Westbrook, 1986)
181. $C_3H_8 + HO_2 = i\text{-}C_3H_7 + H_2O_2$	3.39E12	0.00	17000	1.11E+13	−0.06	8047	(Pitz and Westbrook, 1986)
182. $C_3H_8 + HO_2 = n\text{-}C_3H_7 + H_2O_2$	1.12E13	0.00	19400	3.25E+12	0.00	5991	(Pitz and Westbrook, 1986)
183. $C_3H_8 + CH_4 + i\text{-}C_3H_7$	1.10E15	0.00	25140	2.44E+16	0.05	35034	(Pitz and Westbrook, 1986)
184. $C_3H_8 + CH_3 = CH_4 + n\text{-}C_3H_7$	1.10E15	0.00	25140	2.17E+15	0.10	30579	(Pitz and Westbrook, 1986)
185. $C_3H_8 + C_2H_3 = C_2H_4 + i\text{-}C_3H_7$	1.00E11	0.00	10400	1.65E+13	−0.25	23102	(Pitz and Westbrook, 1986)
186. $C_3H_8 + C_2H_3 = C_2H_4 + n\text{-}C_3H_7$	1.00E11	0.00	10400	1.47E+12	−0.20	18647	(Pitz and Westbrook, 1986)
187. $C_3H_8 + C_2H_5 = C_2H_6 + i\text{-}C_3H_7$	1.00E11	0.00	10400	6.33E+13	−0.29	15148	(Pitz and Westbrook, 1986)
188. $C_3H_8 + C_2H_5 = C_2H_6 + n\text{-}C_3H_7$	1.00E11	0.00	10400	5.62E+12	−0.24	10693	(Pitz and Westbrook, 1986)
189. $C_3H_8 + C_3H_5 = i\text{-}C_3H_7 + C_3H_6$	2.00E11	0.00	16100	5.36E+09	0.76	−821	(Pitz and Westbrook, 1986)
190. $C_3H_8 + C_3H_5 = n\text{-}C_3H_7 + C_3H_6$	7.94E11	0.00	20500	1.89E+09	0.81	−878	(Pitz and Westbrook, 1986)
191. $i\text{-}C_3H_7 = H + C_3H_6$	6.31E13	0.00	36900	2.29E+10	0.60	−2164	(Pitz and Westbrook, 1986)
192. $i\text{-}C_3H_7 + O_2 = C_3H_6 + HO_2$	1.00E12	0.00	5000	4.74E+09	0.31	15970	(Pitz and Westbrook, 1986)
193. $i\text{-}C_3H_7 = CH_3 + C_2H_4$	2.00E10	0.00	29500	4.15E+00	1.95	−1017	(Pitz and Westbrook, 1986)
194. $i\text{-}C_3H_7 + C_3H_8 = n\text{-}C_3H_7 + C_3H_8$	3.02E10	0.00	12900	2.68E+09	0.05	8439	(Pitz and Westbrook, 1986)
195. $n\text{-}C_3H_7 = CH_3 + C_2H_4$	9.55E13	0.00	31000	2.23E+05	1.89	4937	(Pitz and Westbrook, 1986)
196. $n\text{-}C_3H_7 = H + C_3H_6$	1.26E14	0.00	37000	5.15E+11	0.55	2391	(Pitz and Westbrook, 1986)
197. $n\text{-}C_3H_7 + O_2 = C_3H_6 + HO_2$	1.00E12	0.00	5000	5.34E+10	0.26	20425	(Pitz and Westbrook, 1986)
198. $C_3H_6 = C_3H_5 + H$	1.00E13	0.00	78000	8.66E+11	−0.18	−1720	(Pitz and Westbrook, 1986)
199. $C_3H_6 = C_2H_3 + CH_3$	6.31E15	0.00	85800	5.08E+04	2.18	−15000	(Pitz and Westbrook, 1986)
200. $C_3H_6 + H = C_3H_5 + H_2$	5.01E12	0.00	1500	4.14E+11	−0.01	25673	(Pitz and Westbrook, 1986)
201. $C_3H_6 + O = C_2H_5 + HCO$	6.76E04	2.56	−1130	2.96E−03	4.00	23697	(Pitz and Westbrook, 1986)
202. $C_3H_6 + O = CH_3 + CH_3CO$	6.67E04	2.56	−1130	2.45E−02	3.85	32132	(Pitz and Westbrook, 1986)

203.	$C_3H_6 + O = C_2H_4 + CH_2O$	6.76E04	2.56	−1130	9.57E+00	3.56	78072	(Pitz and Westbrook, 1986)
204.	$C_3H_6 + OH = CH_3 + CH_3HCO$	1.00E12	0.00	0	6.08E+09	0.44	18511	(Pitz and Westbrook, 1986)
205.	$C_3H_6 + OH = C_2H_5 + CH_2O$	1.00E12	0.00	0	4.45E+08	0.74	14213	(Pitz and Westbrook, 1986)
206.	$C_3H_6 + OH = C_3H_5 + H_2O$	1.00E13	0.00	3060	3.41E+13	−0.27	43025	(Pitz and Westbrook, 1986)
207.	$C_3H_6 + O_2 = C_3H_5 + HO_2$	1.00E14	0.00	9000	1.13E+14	−0.48	9318	(Pitz and Westbrook, 1986)
208.	$C_3H_6 + CH_3 = C_3H_5 + CH_4$	1.58E12	0.00	8800	1.31E+1	−0.71	35614	(Pitz and Westbrook, 1986)
209.	$C_3H_6 + C_2H_5 = C_3H_5 + C_2H_6$	1.00E11	0.00	9800	2.36E+15	−1.05	31461	(Pitz and Westbrook, 1986)
210.	$C_3H_5 = C_3H_4 + H$	3.98E13	0.00	70000	2.46E+08	1.29	2429	(Pitz and Westbrook, 1986)
211.	$C_3H_5 + H = C_3H_4 + H_2$	1.00E13	0.00	0	5.96E+07	1.46	36318	(Pitz and Westbrook, 1986)
212.	$C_3H_5 + O_2 = C_3H_4 + HO_2$	6.03E11	0.00	10000	4.91E+07	1.00	−7523	(Pitz and Westbrook, 1986)
213.	$C_3H_5 + CH_3 = C_3H_4 + CH_4$	1.00E12	0.00	0	5.97E+10	0.76	38963	(Pitz and Westbrook, 1986)
214.	$C_3H_4 + O = CH_2O + C_2H_2$	1.00E12	0.00	0	3.33E+09	0.65	78363	(Pitz and Westbrook, 1986)
215.	$C_3H_4 + O = HCO + C_2H_3$	1.00E12	0.00	0	5.34E+05	1.30	25615	(Pitz and Westbrook, 1986)
216.	$C_3H_4 + OH = CH_2O + C_2H_3$	1.00E12	0.00	0	5.43E+09	0.60	15002	(Pitz and Westbrook, 1986)
217.	$C_3H_4 + OH = HCO + C_2H_4$	1.00E12	0.00	0	5.57E+10	0.35	32800	(Pitz and Westbrook, 1986)
218.	$C_3H_3 + H(+M) = C_3H_4(+M)$[d]	2.00E13	0.00	0	5.86E+16	−0.53	83967	(Miller *et al.*, 1982)
	Low pressure limit	0.67E19	0.00	0	1.96E+22	−0.53	83967	
	Enhanced third-body efficiencies[e]: H_2/3.3/ H_2O/21/ CO/2/ CO_2/5/							
219.	$C_2H_2 + CH_2 = C_3H_3 + H$	1.00E12	0.00	0	1.23E+17	−1.12	19153	(Miller *et al.*, 1982)

[a] Reaction mechanism rate coefficients in the form $k_f = AT^B \exp(-E_a/RT)$ (units are moles, cubic centimeters, seconds, Kelvins and calories/mole).

[b] Forward rate taken from the reported reference.

[c] Backward rate calculated from forward by equilibrium using the CHEMKIN (Kee *et al.*, 1987) thermodynamic data.

[d] Fall-off reaction in the Lindemann form given the high and low pressure limits.

[e] Only species with non-unity collision efficiency are specified.

TABLE III
Comparison between experimental hydrocarbon/air laminar flame speeds (cm/s), S_u^0, at p = 1 atm and ϕ = 1 with predicted values using the present kinetic scheme

	CH_4	C_2H_6	C_2H_4	C_2H_2
Experimental data[a]	40.2	42.5	65.8	135.4
Present scheme	39.3	42.9[b]	64.0[b]	136.0[b]

[a] As determined by Egolfopoulos *et al.* (1990, 1991).
[b] Calculated with C_3-reactions of Table II.

R106 ($C_2H_3 + H = C_2H_2 + H_2$) was used while the rate of reaction R110 ($C_2H_3 + O_2 = CH_2O + HCO$) was reduced by a factor of four (Egolfopoulos *et al.*, 1990, 1991) from that reported by Slagle *et al.* (1989). Furthermore, the formulation of Stewart *et al.* (1989) for the pressure dependence (SRI fall-off parameters) of the reaction R21 ($CH_4 + M = CH_3 + H + M$) was adopted. Comparisons between experimental and calculated flame speeds for stoichiometric mixtures of CH_4 and the C_2-hydrocarbons with air at 1 atm are shown in Table III and close agreement can be seen. The results of the C_2-hydrocarbons were obtained by also including the C_3-reactions (R172 through R219) reported in Table II. C_3 chemistry has been shown (Egolfopoulos *et al.*, 1990, 1991) to decrease the laminar flame speed of atmospheric, stoichiometric C_2-hydrocarbon/air mixtures by 1.5 to 2.5 cm/s.

Grotheer and Kelm (1989) have recently conducted a detailed numerical study of methanol flames with the latest information of Norton and Dryer (1989) and Tsang (1987), predicting laminar flame speeds of methanol/air mixtures at p = 1 atm and T_u = 298 K conditions. In this study, the one-dimensional, time-dependent flame code of Warnatz (1978) was used and a number of revisions was adopted due to significant overprediction of the flame speeds of rich mixtures. The revised scheme was tested against our experimental data for stoichiometric flames at various initial temperatures using the Sandia flame code (Kee *et al.*, 1985; Grcar *et al.*, 1986), and the results are shown in Figure 11. First, note that while the agreement between experimental and numerical data is good at low temperatures, the temperature dependence is not captured

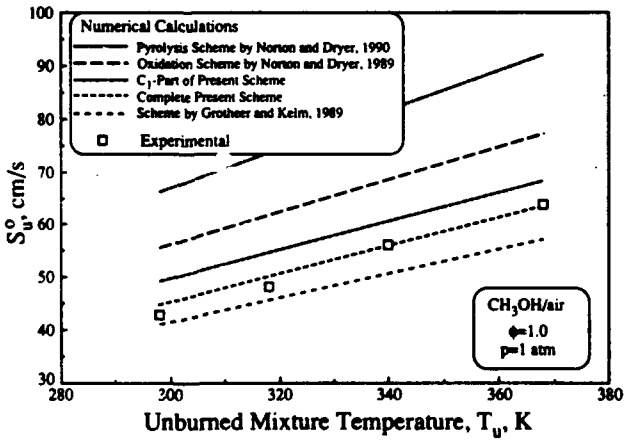

FIGURE 11 Comparison between the experimentally determined S_u^0's of stoichiometric methanol/air flame (ϕ = 1.0) at various T_u's and numerical calculations using the schemes of Grotheer and Kelm (1989), Norton and Dryer (1989, 1990), the C_1 part of the present scheme, and the "full" present scheme.

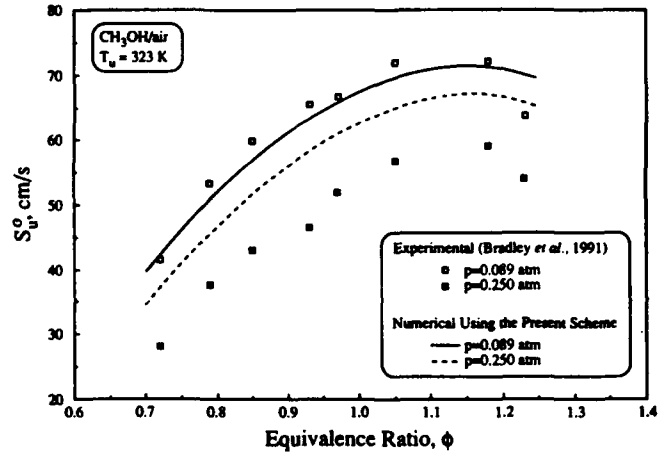

FIGURE 12 Comparison between the experimental S_u^0's of methanol/air mixtures as determined by Bradley *et al.* (1991) at 0.089 and 0.25 atm and numerical calculations using the present scheme.

closely, leading to an underprediction of about 6 cm/s for the $T_u = 368$ K flame. Second, the predicted flame speed for $T_u = 298$ K is close to that reported by Grotheer and Kelm, suggesting that the numerical codes developed by Warnatz and Kee and coworkers lead to similar results for the same kinetic scheme. It may also be noted at this point that during the compilation of the present kinetic scheme the laminar flame speeds were predicted relatively well and the overpredictions as reported by Grotheer and Kelm were not encountered.

In Figure 11 the present experimental data are also compared with the numerical predictions by using the two schemes reported by Norton and Dryer (1989, 1990) on methanol oxidation and pyrolysis. For both cases significant overpredictions are seen. Since these schemes were developed based mainly on flow reactor data, the observed discrepancy demonstrates the importance of validating proposed schemes against experimental data from flames, in which wide variations in temperatures and concentrations are embedded, and the "coupling" of various species through molecular diffusion can result in effects which cannot be adequately captured in a homogeneous system.

In order to quantify the contribution of the C_2 species chemistry on laminar flame propagation, calculations were conducted for the stoichiometric methanol/air flames at various T_u's, both with and without the C_2 chemistry of the present scheme. These results are compared with the experimental data in Figure 11, where it can be seen that the effect of the C_2 chemistry is to slightly reduce the flame speed, by 3–4 cm/s. This effect is due to the fact that with the inclusion of the C_2 chemistry, the CH_3 radicals partially recombine to form C_2H_6 instead of being oxidized to CH_2O or CH_3O which are less stable.

The present scheme was further tested against the new experimental flame speed data as determined by Bradley *et al.* (1991) at 0.089 and 0.25 atm. The comparisons are shown in Figure 12 and it can be seen that although the calculations predict closely the 0.089 atm data, they overpredict the flame speeds at 0.25 atm. The calculations performed by Bradley *et al.* (1991) predicted closely the 0.25 atm data but significantly underpredicted the data at 0.089 atm, indicating that their scheme is slower than the present one. Since Bradley *et al.* (1991) mentioned that there were some uncertainties

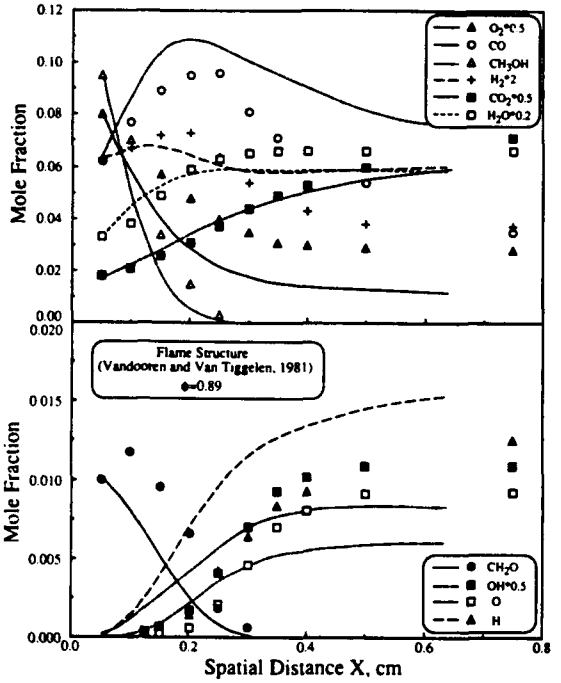

FIGURE 13 Comparison between the experimental (symbols) flame structure as determined by Vandooren and Van Tiggelen (1981) and numerical calculations (lines) using the present scheme. (Flame I: $m'' = 3.302E-03$ gm/sec-cm^2, $\phi = 0.89$, 19.9% CH_3OH, 33.7% O_2, 46.4% Ar, $p = 0.053$ atm; all concentrations on per mole basis).

associated with the measurements, further attempts to assess the cause of these discrepancies were not made.

5 STUDIES BASED ON LAMINAR FLAME STRUCTURES

Since the laminar flame speed is only a global property of the flame, its sensitivity on certain aspects of the flame kinetics can be quite limited. A more stringent test would involve predictions and comparisons of the flame structure, especially the stable and radical species profiles. Among the various experimental studies which have been conducted on low pressure methanol flames using the flat-flame burner technique, the experimental data reported by Vandooren and Van Tiggelen (1981), Pauwels *et al.* (1989, 1990), and Bradley *et al.* (1991) were modeled herein.

In the study by Vandooren and Van Tiggelen (1981), the molecular beam sampling technique, coupled with mass spectrometric detection, were used to measure the concentrations of both stable species and radicals such as H, O, and OH. Consequently, rate coefficients were derived for the reactions of (a) methanol with H and OH, (b) hydroxymethyl with oxygen, and (c) the thermal decomposition of formaldehyde. In the studies by Pauwels *et al.* (1989, 1990), sampling was performed with a quartz probe and the concentrations were determined by using electron spin resonance spectroscopy for H, O, and OH, and gas chromatography for the stable species. These data were tested (Pauwels *et al.*, 1990) against calculations using an updated version of the Westbrook and Dryer mechanism (1979) with 34 reversible

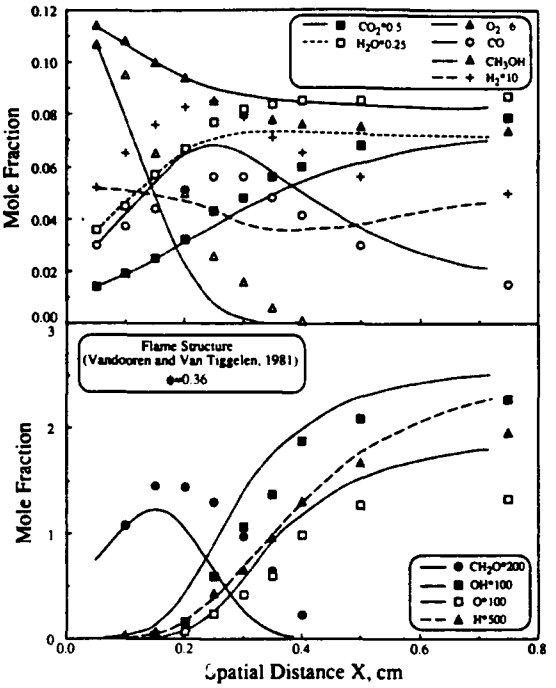

FIGURE 14 Comparison between the experimental (symbols) flame structure as determined by Vandooren and Van Tiggelen (1981) and numerical calculations (lines) using the present scheme. (Flame II: $m^0 = 3.029 \times 10^{-3}$ gm/sec-cm^2, $\phi = 0.36$, 19.4% CH_3OH, 80.6% O_2, $p = 0.053$ atm; all concentrations on per mole basis).

reactions, and it was found that the structure of fuel lean flames was not reproduced accurately. Bradley *et al.* (1991) reported the structure of a moderately-rich flame determined by microprobe for species sampling, gas chromatography for species analysis, and LDV for the flow velocities. A kinetic scheme was also compiled which closely reproduced their measured flame structure but underpredicted the corresponding flame speed by 11 cm/s. In all three studies (Vandooren and Van Tiggelen, 1981; Pauwels *et al.*, 1989, 1990; and Bradley *et al.*, 1991), temperature was measured with thermocouple and corrected for radiative losses. The measurements of Pauwels *et al.* (1989, 1990) had an additional conductive loss to the sampling probe by being adjacent to the thermocouple.

For the modeling of burner-stabilized flames, the Sandia code (Kee *et al.*, 1985; Grcar *et al.*, 1986) was used which can either solve the energy equation or employ a user-specified temperature profile. Experimentally, measurements close to the burner surface can be difficult to obtain and data are typically reported only beyond a certain minimum distance from the burner. For example, in the studies by Vandooren and Van Tiggelen (1981) and Pauwels *et al.* (1989, 1990), the first experimental concentrations were reported at temperatures of ~ 1000 K. Moreover, the use of a thermocouple for temperature measurements can result in locally reduced temperatures and that imposes the constraint of using the experimental temperature profile instead of solving the energy equation. This approach both facilitates the calculations and more accurately simulates the actual experiment since heat losses do not have to be modeled. It must be recognized, however, that by not solving the energy equation the

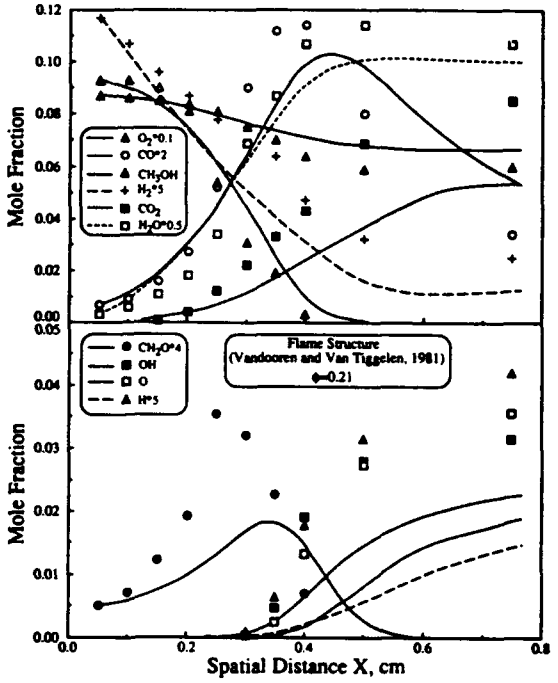

FIGURE 15 Comparison between the experimental (symbols) flame structure as determined by Vandooren and Van Tiggelen (1981) and numerical calculations (lines) using the present scheme. (Flame III: $m^0 = 5.207 \times 10^{-3}$ gm/sec-cm^2, $\phi = 0.21$, 10.9% CH_3OH, 3.2% H_2, 85.9% O_2, $p = 0.053$ atm; all concentrations on per mole basis).

exothermicities of certain reactions are imposed instead of being independently calculated. Furthermore, by using intrusive techniques for flame structure studies there is always the possibility of altering local species concentrations due to interactions with the probe.

In the present investigation, the Sandia code was used with the experimental temperature profile as input for the flames of Vandooren and Van Tiggelen (1981) and Pauwels *et al.* (1989, 1990). The data of Bradley *et al.* (1991) were simulated by also solving for the energy equation since data were reported close to the burner surface and the authors have also modeled the flame as adiabatic. For all cases, at the first computational point the summation of the species mole fractions ranges between 0.95 and 0.99, indicating that all species were mostly accounted for.

Figures 13, 14, and 15 show the comparisons between calculations using the present scheme and the experimental data for flames I, II, and III respectively, as reported by Vandooren and Van Tiggelen (1981), at $p = 0.053$ atm (40 Torr). Flame I is a lean flame ($\phi = 0.89$) with molar concentrations of 19.9% CH_3OH, 33.7% O_2, and 46.4% Ar, and the comparisons are shown in Figure 13. It is seen that in the methanol consumption zone the profiles of all stable species are predicted closely, with the exception of O_2 which is underpredicted. The profiles of H, O, and OH are predicted satisfactorily, but due to uncertainties associated with the measurement of these radicals it is difficult to rigorously assess the validity of the predictions. Flame II is a lean flame ($\phi = 0.36$) with molar concentrations of 19.4% CH_3OH and 80.6% O_2, and the comparisons are shown in Figure 14. The majority of stable species as well

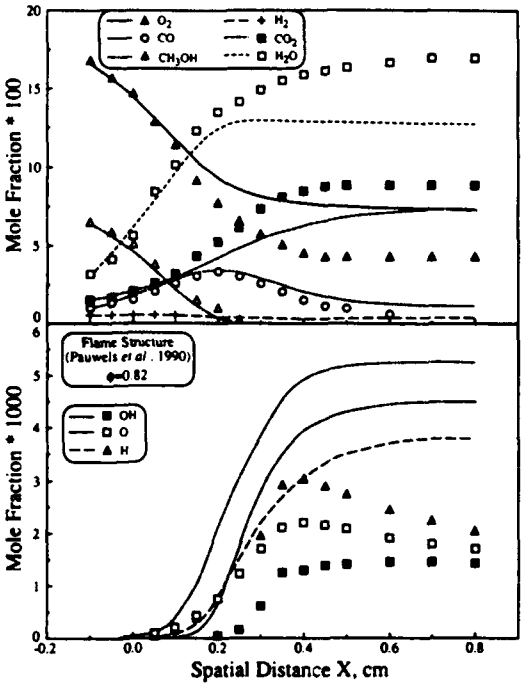

FIGURE 16 Comparison between the experimental (symbols) flame structure as determined by Pauwels *et al.* (1989, 1990) and numerical calculations (lines) using the present scheme. ($m^0 = 2.96 \times 10^{-3}$ gm/sec-cm^2, $\phi = 0.82$, 9.9% CH_3OH, 18.1% O_2, 72.0% N_2, $p = 0.105$ atm; all concentrations on per mole basis).

as H, O, and OH are predicted closely. The exceptions are H_2, which exists in trace amounts, and CH_3OH, whose predicted rate of consumption is somewhat faster than the experimental values. Flame III is a lean flame ($\phi = 0.21$) with molar concentrations of 10.9% CH_3OH, 3.2% H_2, and 85.9% O_2, and the comparisons are shown in Figure 15. All stable species are predicted closely, but the H, O, and OH radicals are significantly underpredicted. The close agreements of the CH_3OH profile for Flames I and III contrast with the discrepancy found in Flame II, suggesting that systematic errors in the methanol consumption reactions cannot be identified through these comparisons.

Figures 16, 17, and 18 compare calculations using the present scheme and the experimental data as reported by Pauwels *et al.* (1989, 1990) for methanol/air flames at $p = 0.105$ atm and equivalence ratios of 0.82, 1.08, and 1.50 respectively. For all cases the stable species are predicted closely within the fuel consumption zone, with the exception of the CH_3OH profile for the $\phi = 1.50$ flame which is "steeper" as compared to that of the experiment. The radical species H, O, and OH, however, are overpredicted and this disagreement is more significant for the H radicals in the $\phi = 1.50$ flame. This is probably the cause for the faster consumption rate of CH_3OH through its reactions, R154 and R155, with H. The location at which radicals start being produced is predicted closer as compared to the calculations of Pauwels *et al.* (1990).

Figure 19 compares calculations using the present scheme and the experimental data as reported by Bradley *et al.* (1991) for a methanol/air flame at $p =$

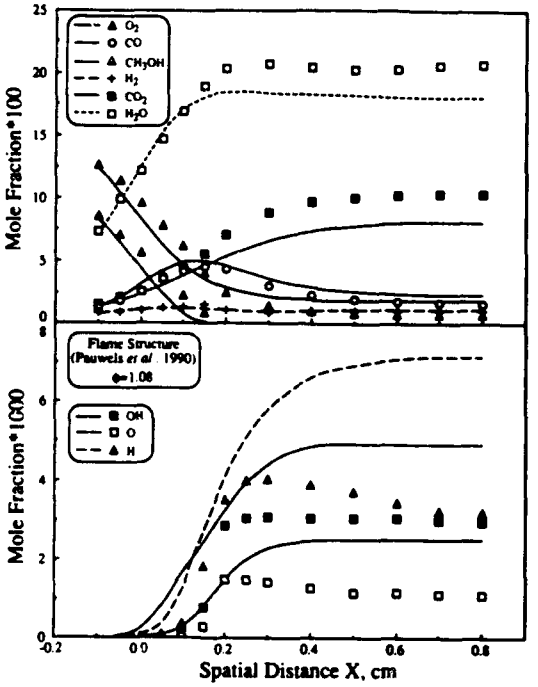

FIGURE 17 Comparison between the experimental (symbols) flame structure profiles as determined by Pauwels *et al.* (1989, 1990) and numerical calculations (lines) using the present scheme. (m^0 = 3.15 × 10^{-3} gm/sec-cm^2, ϕ = 1.08, 12.5% CH_3OH, 17.5% O_2, 70.0% N_2, p = 0.105 atm; all concentrations on per mole basis).

0.089 atm and equivalence ratio ϕ = 1.25. Results show a very close agreement for all species with the exception of some overprediction of the CO after its peak. The present scheme also reproduced very closely both the temperature and flow velocity profiles.

For the comparisons conducted in Figures 13 through 19, a general conclusion is that the present scheme appears to closely predict the flame structure in most cases, capturing the most significant trends of the profiles of the stable species concentrations. In particular, the predicted CO profiles are very close to the experimental data both in magnitude and also in the location of the maximum. Recognizing that CO is an important intermediate and its oxidation can significantly influence global flame properties such as the laminar flame speed, it is reasonable that the accurate prediction of laminar flame speeds by the present kinetic scheme for various conditions correctly accounts for the CO profile. In this study, attempts to obtain better agreements for the H, O, and OH radicals were not made. Experimental measurement of these radicals is much more difficult than that of the stable species because they exist in very small amounts and they are more susceptible to recombinations when intrusive probing techniques are used. Further improvement in studies of this nature would require non-intrusive laser diagnostic techniques to provide concentration and temperature results with higher degrees of confidence and accuracy.

Finally, calculations of the flame structures studied herein were made by using the present scheme and the two different rates (Bowman, 1975; Hess and Tully, 1989) for

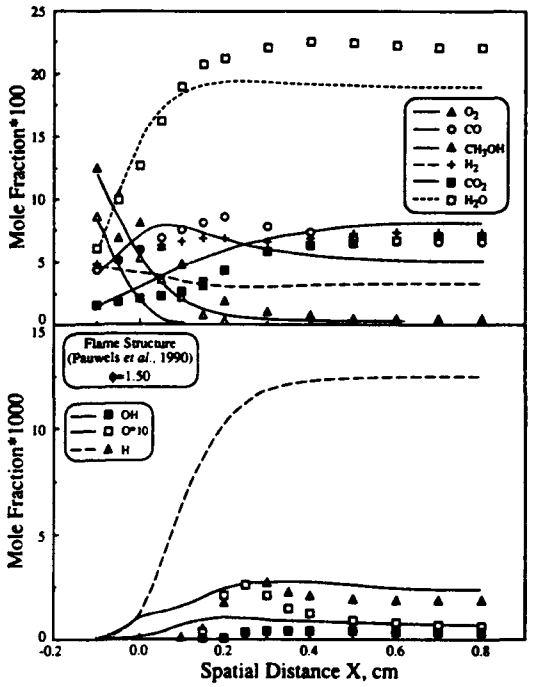

FIGURE 18 Comparison between the experimental (symbols) flame structure as determined by Pauwels *et al.* (1989, 1990) and numerical calculations (lines) using the present scheme. ($m^0 = 2.79 \times 10^{-3}$ gm/sec-cm^2, $\phi = 1.50$, 14.6% CH_3OH, 16.6% O_2, 66.8% N_2, $p = 0.105$ atm; all concentrations on per mole basis).

R157 ($CH_3OH + OH = CH_2OH + H_2O$) and R158 ($CH_3OH + OH = CH_3O + H_2O$) reactions. For all cases it was found that the CH_3OH profile was insensitive to the choice of the rate for R157 and R158, indicating an additional difference between flame studies and pure kinetic studies as it will be further demonstrated in the next section.

6 STUDIES BASED ON FLOW REACTOR RESULTS

The turbulent flow reactor is a valuable experimental technique for the understanding and development of kinetic schemes. Provided that there are no steep concentration gradients in the system, molecular diffusion is negligibly small compared to axial convection and therefore the reaction progress is solely kinetically controlled. The axial distance can be directly converted to the time coordinate through the local flow velocity, and modeling is conducted by solving the time dependent equations of species and energy. The flow reactor operates in temperatures between approximately 1000 and 1200 K, and the system is near-adiabatic before any significant amount of heat is released. Therefore, for the numerical modeling of the flow reactor data, adiabatic solutions were adopted so that the exothermicity and endothermicity of individual reactions are also accounted. This procedure was necessary especially for the oxidation studies in which significant heat is released. In the pyrolysis studies, the system can be considered as practically isothermal since CO is not oxidized. In the

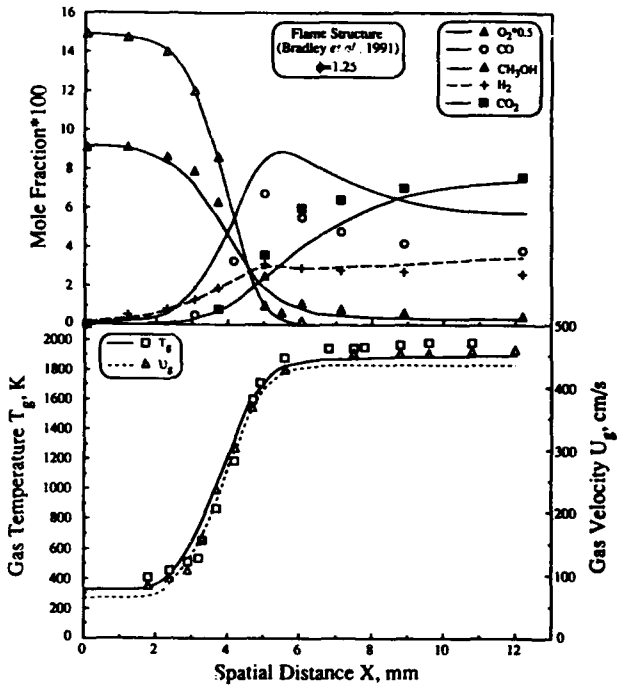

FIGURE 19 Comparison between the experimental (symbols) flame structure as determined by Bradley *et al.* (1991) and numerical calculations (lines) using the present scheme. ($m^0 = 6.41 \times 10^{-3}$ gm/sec-cm^2, $\phi = 1.25$, 14.9% CH_3OH, 17.88% O_2, 67.22% N_2, $p = 0.089$ atm; all concentrations on per mole basis).

present investigation the data of Norton and Dryer (1989) and Aronowitz *et al.* (1977, 1979) for oxidation and pyrolysis conditions were simulated.

It may be recalled from the laminar flame speed studies that modifications of the methanol submechanism were not required since these reactions do not significantly affect propagation. An earlier version of the present mechanism was tested against the oxidation data of Norton and Dryer (1989) by using SENKIN (Lutz *et al.*, 1987) for a constant pressure, adiabatic system which closely resembles the experimental configuration. In these simulations, a discrepancy was found between numerical and experimental results as indicated by a predicted methanol profile which was too "steep" and a temperature increase which was substantially faster as compared to the experimental data. Similar behavior was also observed when modeling the oxidation data of Aronowitz *et al.* (1979).

The observed discrepancies motivated further investigation of the methanol submechanisms of Norton and Dryer (1989, 1990), and the sensitivity of each reaction of CH_3OH, CH_2OH, CH_3O, CH_2O, HCO, HO_2, and H_2O_2 to the fuel decay profile was examined in detail. These species were chosen because they are the important intermediates subsequent to fuel decay, and because they can also significantly influence the production of H and OH radicals. It was consequently identified that the methanol profile is primarily sensitive to the reactions between CH_3OH and OH which produce CH_2OH and CH_3O (reactions R157 and R158 respectively). By examining the reactions controlling the OH production, it was found that by increasing the rate of R11 ($HO_2 + H = H_2 + O_2$) by a factor of 3, improved agreements with the experimental methanol profile were obtained. Reaction R11 provides ter-

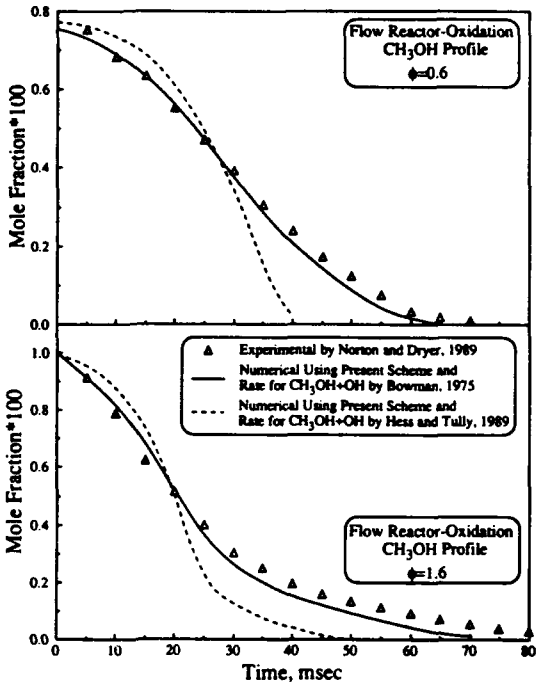

FIGURE 20 Comparison between the experimental (symbols) profiles for CH_3OH at various ϕ's as determined by Norton and Dryer (1989) in a flow reactor, and numerical calculations (lines) using the present scheme with the rate for reaction $CH_3OH + OH$ taken from Hess and Tully (1989) and Bowman (1975).

mination to the system since it does not allow HO_2 to further branch to OH. This modification, however, was not adopted because certain important intermediates such as CH_2O and H_2 were overpredicted by as much as a factor of two, while the O_2 profile was not reproduced satisfactorily and the temperature profile also appeared to have a much wider "plateau" (Norton and Dryer, 1989) as compared to the experiments. Furthermore, it has been shown (Egolfopoulos and Law, 1991) that the low temperature hydrogen chemistry is slow in predicting the laminar flame speeds of very lean hydrogen/air mixtures and this modification would further retard the overall reaction progress. The rates of Hess and Tully (1989) for reactions R157 and R158, used by Norton and Dryer (1990), were measured up to 866 K and are higher than previously recommended rates (Bowman, 1975; Westbrook and Dryer, 1979) for temperatures above 700 K. The branching ratio $CH_2OH : CH_3O$ used by Norton and Dryer (1990) was 1 : 1, as suggested by Hess and Tully, and in the first attempt to improve on the predictions this ratio was varied from 0.2 : 0.8 to 0.8 : 0.2 with the total rate being held constant. That had an effect on the induction time but the slope of the methanol profile remained practically unchanged. The reactor temperature was also varied by ± 15 K, resulting in only minor changes in the predicted slope of the methanol profile. Finally, it was found that a total rate for R157 and R158 smaller by 3.5 times at ~ 1000 K would result in very close agreements for the methanol profiles as well as the other species and temperature. Noting that the rate suggested by Bowman (1975) for high temperatures appears to be almost 3.2 times slower at

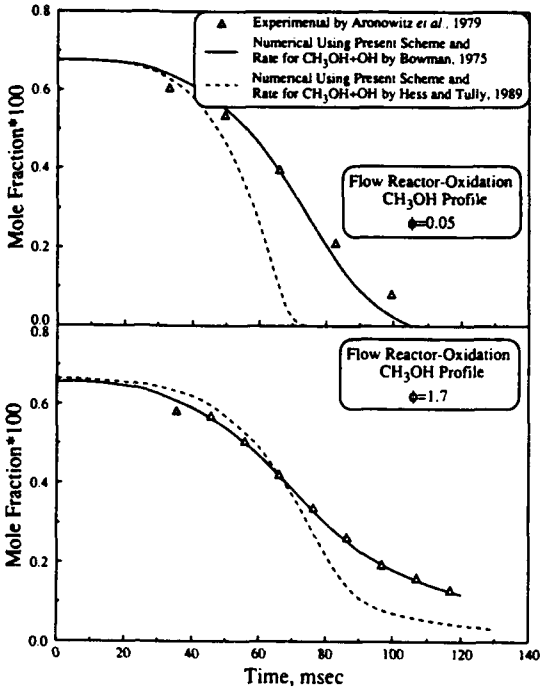

FIGURE 21 Comparison between the experimental (symbols) profiles for CH_3OH at various ϕ's as determined by Aronowitz *et al.* (1979) in a flow reactor and numerical calculations (lines) using the present scheme with the rates for reaction $CH_3OH + OH$ taken from Hess and Tully (1989) and from Bowman (1975).

1000 K. Bowman's rate and a branching ratio of 1 : 1 were subsequently adopted and extensive agreements were obtained for all oxidation data.

In order to demonstrate the effect of these modifications, the experimental data for methanol decay in all oxidation runs studied herein are compared with the predictions of Figures 20 and 21 by using the two rates for R157 and R158. It is clear that significant improvement for lean and rich cases is obtained by using the slower rate. The scheme of Grotheer and Kelm (1989) was also tested against the flow reactor data and it was found that it results in much longer induction times, as compared to the present scheme, as well as unsatisfactory species predictions.

Predictions from calculations by using Bowman's rate (1975) for R157 and R158 are shown in Figures 22 and 26 for various experimental data sets on oxidation. In all cases, due to the uncertainty related to the experimental induction time, the numerical results had to be "time shifted" (Norton and Dryer, 1989, 1990; Norton, 1990) in order to match the experimental data at the 50% fuel decay point; this amount is reported in each figure. The results show that there is good agreement for most of the species until the temperature increases to the point where heat loss to the wall (maintained at $\sim$ 1000 K) and/or molecular diffusion become significant. In this regime the adiabatic, homogeneous model is probably not a good representation of the experimental conditions and thus discrepancies in the CO oxidation region immediately following the fuel consumption zone were not further assessed. For all cases, however, the calculated peak values of CO as well as their locations agree very well with the experimental data. In addition, the present mechanism captures the

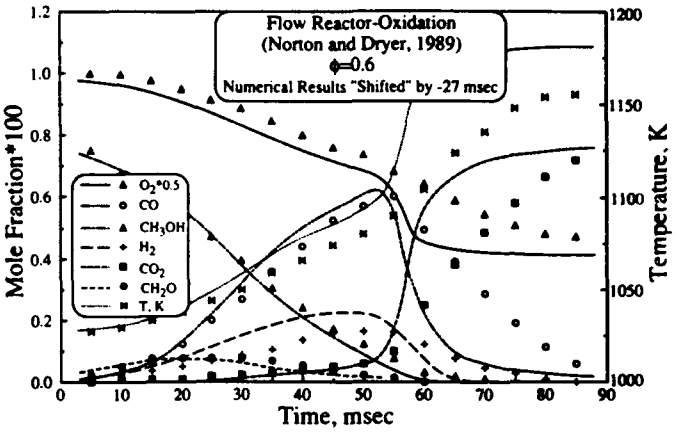

FIGURE 22 Comparison between experimental (symbols) flow reactor oxidation data for $\phi = 0.6$ as determined by Norton and Dryer (1989) and numerical calculations (lines) using the present scheme of Table I. (0.779% CH_3OH, 1.98% O_2, 97.2404% N_2, $T_{in} = 1027$ K, $p_{in} = 1.0$ atm, adiabatic, isobaric; all concentrations on per mole basis).

temperature "plateau" for rich flames as well as the "early" CO_2 production, as first analyzed by Norton and Dryer (1989). It is also important to note the close prediction of the concentration profiles of CH_2O, which is a key species for methanol oxidation.

The present mechanism has been also tested against the pyrolysis flow reactor data of Aronowitz *et al.* (1977) and the results are shown in Figure 27. The numerical solution was obtained for isothermal, constant pressure conditions. The agreements for all species are very close; in particular, the CH_4 profile is predicted closer than that of Norton and Dryer (1990), possibly due to the completeness of the C_1 and C_2 subsets of the present mechanism.

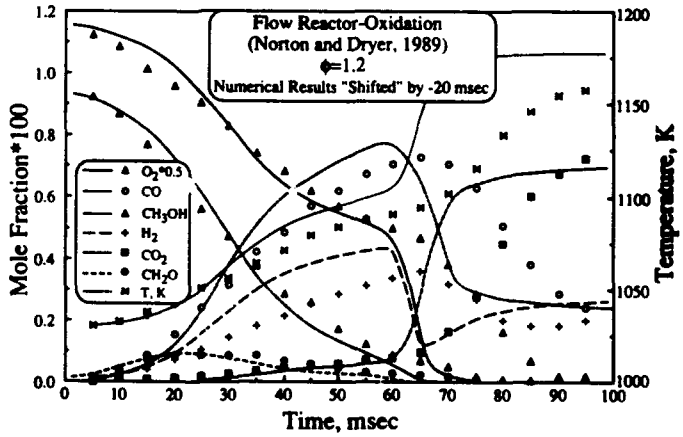

FIGURE 23 Comparison between experimental (symbols) flow reactor oxidation data for $\phi = 1.2$ as determined by Norton and Dryer (1989) and numerical calculations (lines) using the present scheme of Table I. (0.943% CH_3OH, 1.16% O_2, 97.8964% N_2, $T_{in} = 1030$ K, $p_{in} = 1.0$ atm, adiabatic, isobaric; all concentrations on per mole basis).

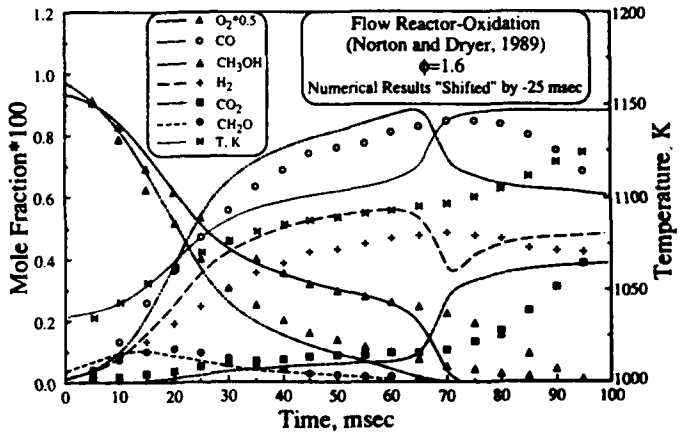

FIGURE 24 Comparison between experimental (symbols) flow reactor oxidation data for $\phi = 1.6$ as determined by Norton and Dryer (1989) and numerical calculations (lines) using the present scheme of Table I. (1.01% CH_3OH, 0.961% O_2, 98.0284% N_2, $T_{in} = 1034$ K, $p_{in} = 1.0$ atm, adiabatic, isobaric; all concentrations on per mole basis).

7 STUDIES BASED ON STATIC REACTOR RESULTS

In order to assess the validity of the present kinetic scheme at lower temperatures, static reactor data were also modeled. An important kinetic difference between the static reactor and other experimental configurations is that lower initial mixture temperatures can be obtained since there is no geometric restrictions for a long induction time. Therefore, the characteristic time scale for the static reactor (sec) can be orders of magnitude greater than the typical time scales for either the flow reactor (msec) or the shock tube (μsec). Experimental studies of methanol pyrolysis and oxidation in static reactors have been conducted by Cathonnet *et al.* (1979, 1982) for various pressures and temperatures; for all experiments the reactor is reported as near

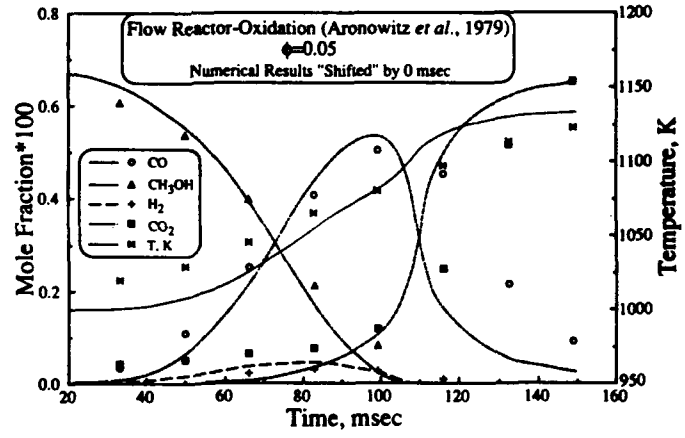

FIGURE 25 Comparison between experimental (symbols) flow reactor oxidation data for $\phi = 0.05$ as determined by Aronowitz *et al.* (1979) and numerical calculations (lines) using the present scheme of Table I. (0.6754% CH_3OH, 20.2613% O_2, 79.0633% N_2, $T_{in} = 1000$ K, $p_{in} = 1.0$ atm, adiabatic, isobaric; all concentrations on per mole basis).

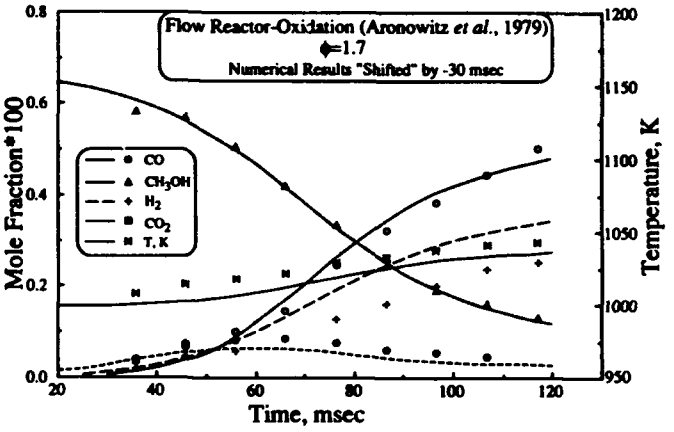

FIGURE 26 Comparison between experimental (symbols) flow reactor oxidation data for $\phi = 1.70$ as determined by Aronowitz *et al.* (1979) and numerical calculations (lines) using the present scheme of Table I. (0.6601% CH_3OH, 0.5824% O_2, 98.7575% N_2, $T_{in} = 998$ K, $p_{in} = 1.0$ atm, adiabatic, isobaric; all concentrations on per mole basis).

isothermal. The modeling was conducted for constant volume and temperature conditions in order to closely simulate the reported experimental configuration, and in no case was it necessary to "time shift" the numerical results in order to match the experimental data.

Two sets of the pyrolysis data from the study of Cathonnet *et al.* (1979) were modeled for the conditions: (a) $p = 0.263$ atm and $T = 918$ K and (b) $p = 0.526$ atm and $T = 973$ K. In both cases the inert gas was nitrogen. Comparisons between calculated and experimental data are shown in Figure 28 and the agreement is within the reported temperature uncertainty of $\pm 1\%$. Norton and Dryer (1990) conducted a sensitivity analysis on the relative effects of separately increasing the rate of reaction R170 ($CH_2OH + CH_2OH = CH_3OH + CH_2O$) by a factor of 5 and varying the temperature by 10 K. It was shown that both adjustments can have similar effects on

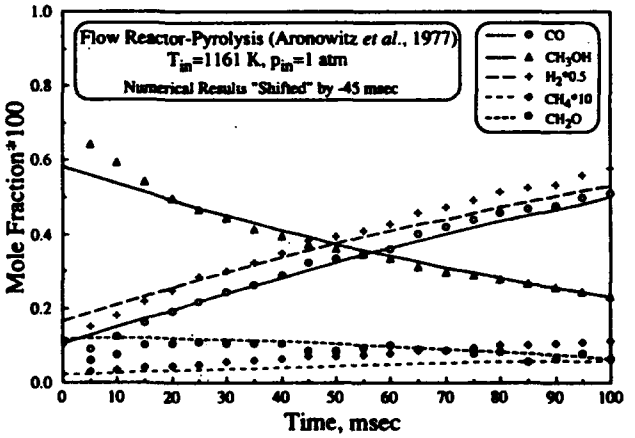

FIGURE 27 Comparison between experimental (symbols) flow reactor pyrolysis data as determined by Aronowitz *et al.* (1977) and numerical calculations (lines) using the present scheme of Table I. (0.815% CH_3OH, 99.19% N_2, $T_{in} = 1.0$ atm, isothermal, isobaric; all concentrations on per mole basis).

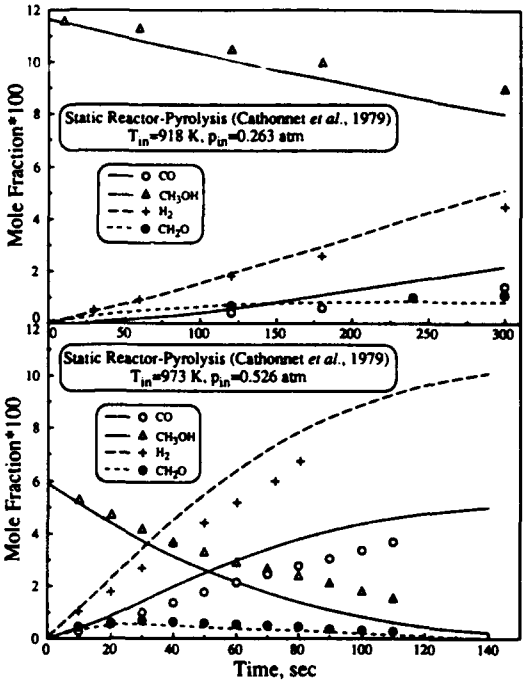

FIGURE 28 Comparison between experimental (symbols) static reactor pyrolysis data as determined by Cathonnet *et al.* (1979) and numerical calculations (lines) using the present scheme of Table I. (Top: 11.6% CH_3OH, 88.4% N_2, T_{in} = 918 K, p_{in} = 0.263 atm, isothermal, isochoric; Bottom: 5.9% CH_3OH, 94.0% N_2, T_{in} = 973 K, p_{in} = 0.526 atm, isothermal, isochoric; all concentrations on per mole basis).

the methanol profile and therefore rate modifications were not made. The present investigation was guided by this approach and further investigation was conducted. It was found that the increase of reaction R170 by a factor of 5 provides in some cases closer agreements for the methanol profile. In general, however, better agreements for the intermediates such as H_2 and CO were provided by using the rate which is reported in Table I and by varying the temperature within its uncertainty range. Since temperature variations alone can account for improved agreement between experimental and numerical results, there is insufficient justification for the increase of the rate of this reaction from the value reported by Norton and Dryer (1990). However, further investigation of this reaction is recommended due to its importance under fuel pyrolysis conditions.

In Figures 29 and 30 experimental oxidation data from the study of Cathonnet *et al.* (1982) are compared with predictions and satisfactory agreements can be seen. The system temperature was varied by $\pm 1\%$ in order to investigate the sensitivity of the intermediates such as H_2 and CO to temperature variations. It was found that improved agreements could be obtained within the range of the temperature uncertainty. Thus, modifications were again not warranted. In general, the static reactor data appear to be sensitive to the reactor temperature uncertainty.

Additional modeling runs were also conducted for the experimental oxidation data by using the rate of Hess and Tully (1989) for reactions R157 and R158. In all cases, the predicted methanol profiles were found to be steeper than the experimental data, again indicating the need for slower rates for these important reactions.

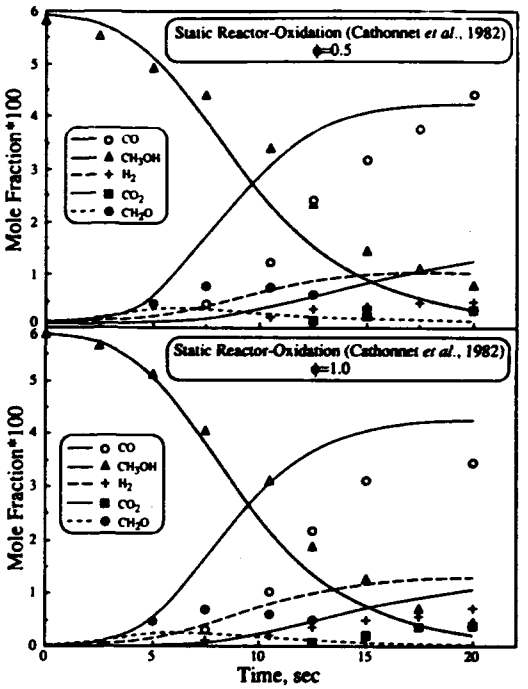

FIGURE 29 Comparison between experimental (symbols) static reactor oxidation data for $\phi = 0.5$ and $\phi = 1.0$ as determined by Cathonnet *et al.* (1982) and numerical calculations (lines) using the present scheme of Table I. (Top: 5.82% CH_3OH, 17.69% O_2, 76.49% N_2, $\phi = 0.5$, $T_{in} = 823$ K, $p_{in} = 0.263$ atm, isothermal, isochoric; Bottom: 5.89% CH_3OH, 8.78% O_2, 85.33% N_2, $\phi = 1.0$, $T_{in} = 823$ K, $p_{in} = 0.263$ atm, isothermal, isochoric; all concentrations on per mole basis).

8 STUDIES BASED ON SHOCK TUBE RESULTS

Reactor-type experiments provide information for the low- and intermediate-temperature regimes, typically between 700 K and 1200 K. Shock tube studies complement these experiments by operating at the higher temperature range of 1500 K to 2500 K, which is of significant relevance to high-temperature combustion.

The present methanol mechanism was tested against the high temperature experimental results obtained from the studies of Bowman (1975) and Cribb *et al.* (1984) for oxidation and pyrolysis conditions respectively. In both investigations the measurements were conducted behind reflected shock waves. This configuration was numerically simulated as an adiabatic, constant volume system, which allows for both temperature and pressure increases during the course of the reaction. Furthermore, the numerical results did not require "time shifting" in order to match the experimental data. The temperature uncertainty for both experiments was reported as ± 50 K; the sensitivity of the predicted properties on this uncertainty has been examined in all cases.

In Figure 31 the pyrolysis experimental data of Cribb *et al.* (1984) at 2000 K and 0.354 atm are compared with the numerical predictions. In general, the predictions were improved by decreasing the temperature to 1950 K, a finding which is in agreement with that reported by Norton and Dryer (1990).

For methanol oxidation conditions, the experimental data of Bowman (1975) were

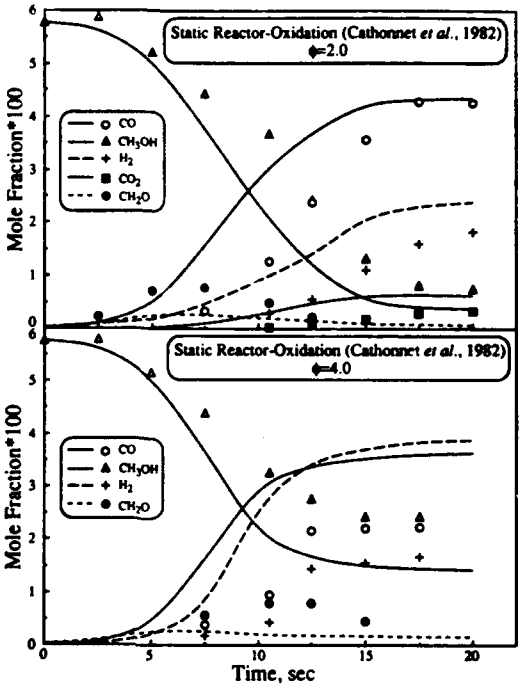

FIGURE 30 Comparison between experimental (symbols) static reactor oxidation data for $\phi = 2.0$ and $\phi = 4.0$ as determined by Cathonnet *et al.* (1982) and numerical calculations (lines) using the present scheme of Table I. (Top: 5.78% CH_3OH, 4.36% O_2, 89.86% N_2, $\phi = 2.0$, $T_{in} = 823$ K, $p_{in} = 0.263$ atm, isothermal, isochoric; Bottom: 5.78% CH_3OH, 2.13% O_2, 92.09% N_2, $\phi = 4.0$, $T_{in} = 823$ K, $p_{in} = 0.263$ atm, isothermal, isochoric; all concentrations on per mole basis).

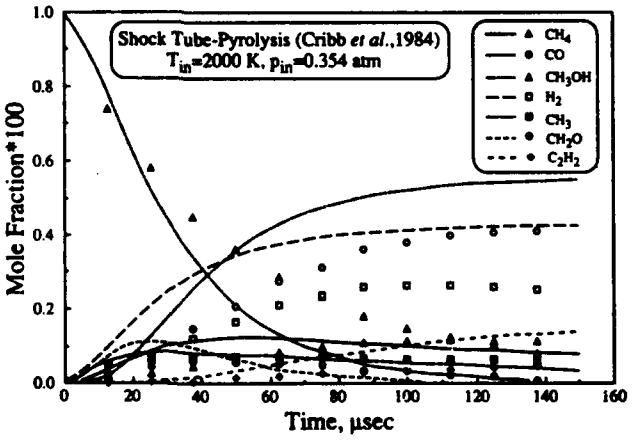

FIGURE 31 Comparison between experimental (symbols) shock tube pyrolysis data as determined by Cribb *et al.* (1984) and numerical calculations (lines) using the present scheme of Table I. (1.0% CH_3OH, 92.18% Ne, 1.0% Ar, 6.0% H_2, $T_{in} = 2000$ K, $p_{in} = 0.354$ atm, adiabatic, isochoric; all concentrations on per mole basis).

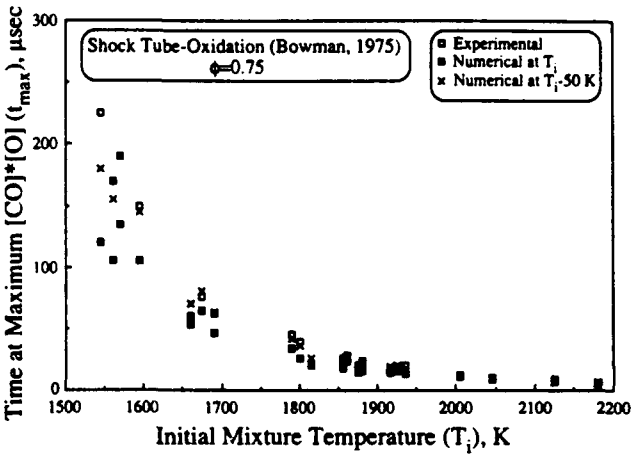

FIGURE 32 Comparison between experimental shock tube oxidation data for $\phi = 0.75$ as determined by Bowman (1975) and numerical calculations using the present scheme of Table I.

modeled. The parameter of interest is t_{max}, which is the time interval between the instants when the reflected shock heats up the mixture and when the product of the [O] and [CO] concentrations reaches a maximum. This parameter can be conveniently measured using optical methods (Bowman, 1975) and has been determined under a variety of conditions. All oxidation conditions reported by Bowman were modeled and close agreements between predicted and experimental values of t_{max} were found within the stated ± 50 K temperature uncertainty. The effect of this uncertainty was greater in the lower temperature regime (1550–1750 K) than for temperatures above 1800 K. Representative results for mixtures of $CH_3OH/O_2/Ar$ for lean ($\phi = 0.75$) and rich ($\phi = 6.00$) conditions are shown in Figures 32 and 33 respectively. The results indicate the discrepancies at low temperatures as well as the potential improvements obtained by varying the temperature within the ± 50 K range. Similar behavior has been observed for all mixtures.

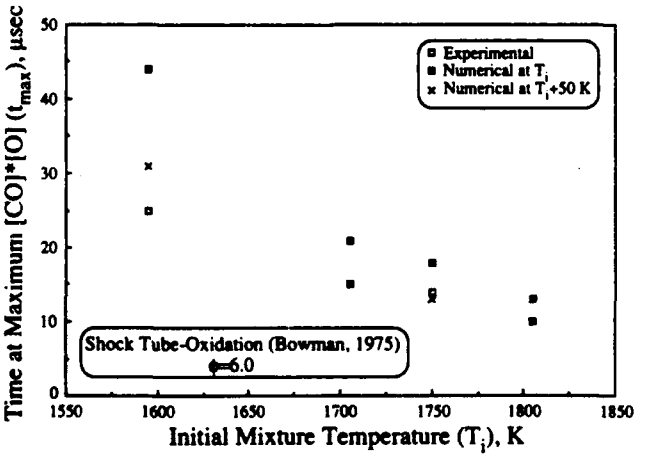

FIGURE 33 Comparison between experimental shock tube oxidation data for $\phi = 6.0$ as determined by Bowman (1975) and numerical calculations using the present scheme of Table I.

In summary, given the temperature uncertainty in the shock tube data, the present scheme is able to predict well the experimental data in all cases by simply varying the temperature within the stated error limits. Because of this agreement, further constraints and/or modifications of individual reactions are not necessary.

9 CONCLUDING REMARKS

In the present investigation, two major objectives were accomplished. The first is the experimental determination of stretch-free laminar flame speed data for atmospheric methanol/air mixtures using the counterflow technique. These data were obtained for various mixture initial temperatures and stoichiometries ranging from very lean to very rich, and can be used with confidence for the validation of methanol kinetics as well as for practical applications. The second objective is the compilation of a methanol kinetic scheme by simultaneously testing it against experimental data for flame speeds, flame structure, flow and static reactors, and shock tubes. The present scheme is also internally consistent by closely predicting laminar flame speeds of mixtures of CH_4 and the C_2-hydrocarbons with air measured in previous investigations.

The modeling of various experimental configurations provided complementary information on the kinetics which are essential for the comprehensive validation of the mechanism. This approach leads to the observation that a rate slower than that reported recently by Hess and Tully (1989) is needed for the $CH_3OH + OH \rightarrow$ Products reaction in order to accurately model both flow and static reactor oxidation data. Such an observation could not be obtained from studies on laminar flames speeds alone. However, the possibility that certain reactions or combinations of reactions produce excess OH in the fuel consumption zone cannot be ruled out even though the present investigation could not identify them. Furthermore, the present kinetic scheme was also used to identify sensitivities and species consumption paths in methanol flames, and to quantitatively demonstrate the differences in formaldehyde and C_2-hydrocarbons production between methanol and methane flames.

The problem of validating rates of crucial reactions with high degree of confidence is, however, far from being closed. In the present investigation, it was shown that the temperature uncertainty for static reactors and shock tubes is sufficiently large that the validity of certain rates simply can not be assessed. Furthermore, uncertainties associated with the rates of methanol reactions and branching ratios, as well as the thermal decompositions of CH_2OH and CH_3O, leave substantial room for further investigation. Some of these issues can be clarified by studying systems at high pressures at which deficiencies in our knowledge of thermal decomposition reactions can be rectified.

Finally, it must also be cautioned that although extensive agreements were obtained in the present investigation, the reported kinetics might not be able to predict methanol oxidation and pyrolysis properties when burning conditions deviate substantially from the present range of conditions. The present kinetic scheme, however, does form a useful starting point from which further investigations can be conducted.

ACKNOWLEDGEMENTS

This research was supported in part by the Army Research Office and the Air Force Office of Scientific Research. It is a pleasure to acknowledge the stimulating discussions with and constructive comments from Professor F. L. Dryer and Drs. K. Brezinsky, T. S. Norton, W. Tsang, R. A. Yetter, and C. K. Westbrook.

REFERENCES

Akrick, R., Vovelle, C., and Delbourgo, R. (1978). Flame Profiles and Combustion Mechanisms of Methanol-Air Flames Under Reduced Pressure. *Combust. Flame* **32**, 171.

Andersson, L. L., Christenson, B., Hoglund, A., Olsson, J. O., and Rosengren, L. G. (1984). Structure of Premixed Laminar Methanol-Air Flames: Experimental and Computational Results. *Prog. in Astronautics and Aeronautics* **95**, 164.

Aronowitz, D., Naegli, D. W., and Glassman, I. (1977). Kinetics of the Pyrolysis of Methanol. *J. Phys. Chem.* **81**, 2555.

Aronowitz, D., Santoro, R. J., Dryer, F. L., and Glassman, I. (1979). Kinetics of the Oxidation of Methanol: Experimental Results Semi-Global Modeling and Mechanistic Concepts. *Seventeenth Symposium (International) on Combustion*, Combustion Institute, p. 633.

Bowman, C. T. (1975). A Shock Tube Investigation of the High-Temperature Oxidation of Methanol. *Combust. Flame* **25**, 343.

Bradley, D., Dixon-Lewis, G., Habik, E-D., Kwa, L. K., and El-Sherif, S. (1991). Laminar Flame Structure and Burning Velocities of Premixed Methanol-Air. *Combust. Flame* **85**, 105.

Cathonnet, M., Boettner, J. C., and James, H. (1979) Étude Expérimentale et Simulation de la Pyrolyse du Méthanol. *J. de Chimie Physique* **76**, 183.

Cathonnet, M., Boettner, J. C., and James, H. (1982). Etude de L'Oxydation et de L'Auto-Inflammation du Méthanol Dans le Domaine de Temperatures 500-600°C. *J. de Chimie Physique* **79**, 475.

Cribb, P. H., Dove, J. E., and Yamazaki, S. (1984). A Shock Tube Study of Methanol Pyrolysis. *Twentieth Symposium (International) On Combustion*, Combustion Institute, p. 779.

Dagaut, P., Cathonnet, M., Boettner, J. C., and Gailklard, F. (1988). Kinetic Modeling of Ethylene Oxidation. *Combust. Flame* **71**, 295.

de Wilde, E. and Van Tiggelen (1968). Burning Velocities in Mixtures of Methyl Alcohol, Formaldehyde, or Formic Acid With Oxygen. *Bull. Soc. Chim. Belges* **77**, 67.

Dove, J. E. and Warnatz, J. (1983). Calculation of Burning Velocity and Flame Structure in Methanol-Air Mixtures. *Ber. Bunsenges. Phys. Chem.* **87**, 1040.

Egolfopoulos, F. N., Cho, P., and Law, C. K. (1989). Laminar Flame Speeds of Methane-Air Mixtures Under Reduced and Elevated Pressures. *Combust. Flame* **76**, 375.

Egolfopoulos, F. N., Zhu, D. L., and Law, C. K. (1990). Laminar Flame Speeds of Mixtures of C_2-Hydrocarbons with Oxygen and Nitrogen. *MAE Report 1891*, Department of Mechanical and Aerospace Engineering, Princeton University.

Egolfopoulos, F. N. and Law, C. K. (1991). An Experimental and Computational Study of the Burning Rates of Ultra-Lean to Moderately-Rich H_2/O_2N_2 Laminar Flames with Pressure Variations. *Twenty-Third Symposium (International) on Combustion*, Combustion Institute, p. 333.

Egolfopoulos, F. N., Zhu, D. L., and Law, C. K. (1991). Experimental and Numerical Determination of Laminar Flame Speeds: Mixtures of C_2-Hydrocarbons with Oxygen and Nitrogen. *Twenty-Third Symposium (International) on Combustion*, Combustion Institute, p. 471.

Gibbs, G. J. and Calcote, H. F. (1959). Effect of Molecular Structure on Burning Velocity. *J. Chem. Eng. Data* **4**, 226.

Glarborg, P., Miller, J. A., and Kee, R. J. (1986). Kinetic Modeling and Sensitivity Analysis of Nitrogen Oxide Formation in Well-Stirred Reactors. *Combust. Flame* **65**, 177.

Gordon, S. and McBride, B. J. (1971). Computer Program for Calculation of Complex Chemical Equilibrium Compositions, Rocket Performance, Incident and Reflected Shocks and Chapman-Jauguet Detonations. *NASA SP-273*.

Grcar, J. F., Kee, R. J., Smooke, M. D., and Miller, J. A. (1986). A Hybrid Newton/Time-Integration Procedure for the Solution of Steady, Laminar, One-Dimensional, Premixed Flames. *Twenty-First Symposium (International) on Combustion*, Combustion Institute, p. 1773.

Grotheer, H-H. and Kelm, S. (1989). Elementary Reactions in the Methanol Oxidation System. Implications on the Modeling of Laminar Burning Velocities. *Proceedings of the III Int. Seminar on Flame Structure*, Sept. 18-22, Alma-Ata, USSR.

Gülder, Ö. L. (1982). Laminar Burning Velocities of Methanol, Ethanol and Isooctane-Air Mixtures. *Nineteenth Symposium (International) on Combustion*, Combustion Institute, p. 275.

Henderson, H. T. and Hill, G. R. (1956). A Kinetic Study of Methyl Chloride Combustion. *J. Phys. Chem.* **60**, 874.

Hennessy, R. J., Robinson, C., and Smith, D. B. (1986). A Comparative Study of Methane and Ethane Flame Chemistry by Experiment and Detailed Modelling. *Twenty-First Symposium (International) on Combustion*, Combustion Institute, p. 761.

Hess, W. P and Tully, F. P. (1989). Hydrogen-Atom Abstraction from Methanol by OH. *J. Phys. Chem.* **93**, 1944.

Hirano, M., Oda, K., Hirano, T., and Akita, K. (1981). Burning Velocities of Methanol-Air-Water Gaseous Mixtures. *Combust. Flame* **40,** 341.

Hsu, K.-J., Anderson, S. M., Durant, J. L., and Kaufman, F. (1989). Rate Constants for H + O_2 + M from 298 to 639 K for M = He, N_2 and H_2O. *J. Phys. Chem.* **93,** 1018.

Kee, R. J., Warnatz, J., and Miller, J. S. (1983). A FORTRAN Computer Code Package for the Evaluation of Gas-Phase Viscosities, Conductivities, and Diffusion Coefficients. *Sandia Report SAND83-8209.*

Kee, R. J., Grcar, J. F., Smooke, M. D., and Miller, J. A. (1985). A Fortran Program for Modeling Steady Laminar One-Dimensional Premixed Flames. *Sandia Report SAND85-8240.*

Kee, R. J., Rupley, F. M., and Miller, J. A. (1987). The CHEMKIN Thermodynamic Data Base. *Sandia Report SAND87-8215.*

Kee, R. J., Rupley, F. M., and Miller, J. A. (1989a). Chemkin-II: A Fortran Chemical Kinetics Package for the Analysis of Gas-Phase Chemical Kinetics. *Sandia Report SAND89-8009.*

Kee, R. J., Miller, J. A., Evans, G. H., and Dixon-Lewis, G. (1989b). A Computational Model of the Structure and Extinction of Strained, Opposed Flow, Premixed Methane–Air Flames. *Twenty-Second Symposium (International) on Combustion,* Combustion Institute, p. 1479.

Law, C. K. (1989). Dynamics of Stretched Flames. *Twenty-Second Symposium (International) on Combustion,* Combustion Institute, p. 1381.

Lutz, A. E., Kee, R. J., and Miller, J. A. (1987). SENKIN: A Fortran Program for Predicting Homogeneous Gas Phase Chemical Kinetics with Sensitivity Analysis. *Sandia Report SAND87-8248.*

Metghalchi, M. and Keck, J. C. (1982). Burning Velocities of Mixtures of Air with Methanol, Isooctane, and Indolene at High Pressure and Temperature. *Combust. Flame* **48,** 191.

Miller, J. A., Mitchell, R. E., Smooke, M. D., and Kee, R. J. (1982). Toward a Comprehensive Chemical Kinetic Mechanism for the Oxidation of Acetylene: Comparison of Model Predictions with Results from Flame and Shock Tube Experiments. *Nineteenth Symposium (International) on Combustion,* Combustion Institute, p. 181.

Norton, T. S. and Dryer, F. L. (1989). Some New Observations on Methanol Oxidation Chemistry. *Comb. Sci. Tech.* **63,** 107.

Norton, T. S. and Dryer, F. L. (1990). Toward a Comprehensive Mechanism for Methanol Pyrolysis. *Int. J. Chem. Kinet.* **22,** 219.

Norton, T. S. (1990). The Combustion Chemistry of Simple Alcohol Fuels. *Ph.D. Thesis,* Department of Mechanical and Aerospace Engineering, Princeton University, Princeton, NJ.

Olsson, J. O., Karlsson, L. S., and Anderson, L. L. (1986). Addition of Water to Premixed Laminar Methanol-Air Flames: Experimental and Computational Results. *J. Phys. Chem.* **90,** 1458.

Olsson, J. O., Olsson, I. B. M., and Andersson, L. L. (1987). Lean Premixed Laminar Methanol Flames: A Computational Study. *J. Phys. Chem.* **91,** 4160.

Pauwels, J. F., Carlier, M., Devolder, P., and Sochet, L. R. (1989). Experimental and Numerical Analysis of a Low Pressure Stoichiometric Methanol–Air Flame. *Comb. Sci. Tech.* **64,** 97.

Pauwels, J. F., Carlier, M., Devolder, P., and Sochet, L. R. (1990). Influence of Equivalence Ratio on the Structure of Low-Pressure Mechanol–Air Flames. *Combust. Flame* **82,** 163.

Pitz, W. A. and Westbrook, C. K. (1986). Chemical Kinetics of the High Pressure of *n*-Butane and Its Relation to Engine Knock. *Combust. Flame* **63,** 113.

Roth, P. and Just, T. (1985). Kinetics of the High Temperature, Low Concentration CH_4 Oxidation Verified by H and O Atom Measurements. *Twentieth Symposium (International) on Combustion,* Combustion Institute, p. 807.

Slack, M. W. (1977). Rate Coefficient for H + O_2 + M = HO_2 + M Evaluated from Shock Tube Measurements of Induction Times. *Combust. Flame* **28,** 241.

Slagle, I. R., Park, J-Y., Heaven, M. C., and Gutman, D. (1984). Kinetics of Polyatomic Free Radicals Produced by Laser Photolysis. 3. Reaction of Vinyl Radicals with Molecular Oxygen. *J. Amer. Chem. Soc.* **106,** 4356.

Sloane, T. M. (1989). Ignition and Flame Propagation Modeling With an Improved Methane Oxidation Mechanism. *Comb. Sci. Tech.* **63,** 287.

Stewart, P. H., Rothem, T., and Golden, D. (1989). Tabulation of Rate Constants for Combustion Modeling. *Twenty-Second Symposium (International) On Combustion,* Combustion Institute, p. 943.

Timonen, R. S., Ratajczak, E., and Gutman, D. (1988). Kinetics of the Reactions of the Formyl Radical with Oxygen, Nitrogen Dioxide, Chlorine, and Bromine. *J. Phys. Chem.* **92,** 651.

Tsang, W. and Hampson, R. F. (1986). Chemical Kinetic Data Base for Combustion Chemistry. Part I. Methane and Related Compounds. *J. Phys. Chem. Ref. Data* **15,** 1087.

Tsang, W. (1987). Chemical Kinetic Data Base for Combustion Chemistry. Part 2. Methanol. *J. Phys. Chem. Ref. Data* **16,** 471.

Vandooren, J. and Van Tiggelen, P. J. (1981). Experimental Investigation of Methanol Oxidation in Flames: Mechanisms and Rate Constants of Elementary Steps. *Eighteenth Symposium (International) on Combustion,* Combustion Institute, p. 473.

Warnatz, J. (1978). Calculation of the Structure of Laminar Flat Flames I: Flame Velocity of Freely Propagating Ozone Decomposition Flames. *Ber. Bunsenges. Phys. Chem.* **82,** 193.

Warnatz, J. (1984a). Rate Coefficients in the C/H/O System. *Combustion Chemistry* (W. C. Gardiner, Ed.), Chap. 5, Springer-Verlag, NY.

Warnatz, J. (1984b). Chemistry of High Temperature Combustion of Alkanes up to Octane *Twentieth Symposium (International) on Combustion*, Combustion Institute, p. 845.

Westbrook, C. K. and Dryer, F. L. (1979). A Comprehensive Mechanism for Methanol Odixation. *Comb. Sci. Tech.* **20,** 125.

Westbrook, C. K. (1980). Inhibition of Laminar Methane–Air and Methanol–Air Flames by Hydrogen Bromide. *Comb. Sci. Tech.* **23,** 191.

Westbrook, C. K. and Dryer, F. L. (1980). Prediction of Laminar Flame Properties of Methanol–Air Mixtures. *Combust. Flame* **37,** 171.

Wiser, W. H. and Hill, G. R. (1955). A Kinetic Comparison of the Combustion of Methyl Alcohol and Methane. *Fifth Symposium (International) on Combustion*, Combustion Institute, p. 553.

Wu, C. K. and Law, C. K. (1985). On the Determination of Laminar Flame Speeds from Stretched Flames. *Twentieth Symposium (International) on Combustion*, Combustion Institute, p. 1941.

Yetter, R. A., Dryer, F. L., and Rabitz, H. (1990). A Comprehensive Reaction Mechanism for Carbon Monoxide/Hydrogen/Oxygen Kinetics. To appear in *Comb. Sci. Tech.*

Yu, G., Law, C. K., and Wu, C. K. (1986). Laminar Flame Speeds of Hydrocarbon + Air Mixtures with Hydrogen Addition. *Combust Flame* **63,** 339.

Zhu, D. L., Egolfopoulos, F. N., and Law, C. K. (1989). Experimental and Numerical Determination of Laminar Flame Speeds of Methane/(Ar N_2, CO_2)–Air Mixtures as Function of Stoichiometry, Pressure, and Flame Temperature. *Twenty-Second Symposium (International) on Combustion*, Combustion Institute, p. 1537.